Brain Microvascular Endothelial Cells-Derived HMGB1 Facilitates Monocyte Transendothelial Migration Favoring JEV Neuroinvasion

Song-Song Zou
Huazhong Angricultural University
Qing-Cui Zou
Huazhong Angricultural University
Wen-Jing Xiong
Huazhong Angricultural University
Ning-Yi Cui
Huazhong Angricultural University
Ke Wang
Huazhong Angricultural University
Hao-Xuan Liu
Huazhong Agricultural University
Wen-Juan Lou
Huazhong Angricultural University
Doaa Higazy
Huazhong Angricultural University
Hao-Wei Chen
Huazhong Angricultural University
Ya-Ge Zhang
Huazhong Angricultural University
Min Cui (cuimin@mail.hzau.edu.cn)
Huazhong Agriculture University https://orcid.org/0000-0001-9691-033X

Research

Keywords: JEV, HMGB1, Monocyte, Blood-brain barrier, Adhesion, Transendothelial migration, “Trojan horse” pathway, Neuroinvasion

Posted Date: November 19th, 2020

DOI: https://doi.org/10.21203/rs.3.rs-108411/v1

Abstract

Background: Infection with the Japanese encephalitis virus (JEV) induced high morbidity and mortality, even caused permanent neurological sequelae. However, the pathways and mechanisms of JEV invasion into the central nervous system (CNS) remain elusive. It is confirmed that extracellular HMGB1 facilitates immune cells transendothelial migration. Furthermore, it is observed that the migration of immune cells into the CNS dramatically increased during JEV infection which may benefit to viral clearance, but paradoxically accompanied by the expedite onset of Japanese encephalitis (JE) in advance. Thus, exploration of JEV neuroinvasion pathways is important for pathogenesis and prevention of JE.

Methods: Brain microvascular endothelial cells were utilized for the detection of HMGB1 release in vitro. The blood-brain barrier (BBB) monolayer model (brain microvascular endothelial cells) and recombinant HMGB1 were applied for the measurement of endothelial cell activation and cells adhesion, the integrity of the BBB and the interaction with the immune cells. A genetically modified JEV expressing EGFP (EGFP-JEV) was used to trace the transmigration of JEV-infected immune cells crossing the BBB to mimic the process of neuroinfection.

Results: JEV has the characteristic of neurotropism, causing HMGB1 released from BMEC and increasing adhesion molecules. BEMC-derived HMGB1 enhances leukocyte-endothelium adhesion, facilitating the transendothelial migration of JEV-infected monocytes across the BBB entry into the CNS. Thus, JEV successfully utilized the monocyte as a “Trojan horse” to spread the virus to the brain, expanding the brain infection, leading the acceleration of JE onset.

Conclusion: JEV-infected monocytes, acting as “Trojan horse”, migrate to the brain, which was facilitated by BMEC-derived HMGB1, contributing to JEV neuroinvasion, and leading neuroinflammation and pathological changes of JE.

Background

Japanese Encephalitis Virus (JEV) is a mosquito-borne, single-stranded positive-sense RNA virus, which is classified within the genus Flavivirus of the family Flaviviridae [1]. JEV is an epidemic virus in the south and eastern regions of Asia, which mainly infects children and infants [1, 2]. Approximately, twenty percent of Japanese encephalitis (JE) patients end up mortal, and about 50% of survivors showed permanent neuropsychiatric sequelae, such as altered sensorium, seizures, movement disorders, and paralysis [1-4]. A recent study has shown that JEV infection is associated with Guillain-Barre syndrome [5]. It was previously that numerous neurotropic pathogens could cause fluctuation to the blood-brain barrier (BBB) such as West Nile virus (WNV), lymphocytic choriomeningitis virus (LCMV), dengue virus (DENV) [6, 7]. Pathologically, it is suggested that the BBB breakdown has a conclusive correlation with neuroinflammation during JEV infection [8]. Currently, there are no known effective therapeutics against JE yet [1, 4, 9]. Hence, it is critical to investigate the pathways and mechanisms of JEV neuroinvasion.

As a dynamic interface of the CNS, the BBB is composed of closely-packed fenestrated brain microvascular endothelial cells (BMECs), assisted with pericytes, astrocytes end-feet, neurons and the extracellular matrix [6, 10, 11]. Moreover, associated intracellular cytoskeleton endowed the features of BBB that manage the transport and metabolism between the circulatory system and the brain as a physical and physiological barrier, restricting the infiltration of immune cells into the brain [8, 10, 11]. The monolayer transwell model was accepted to mimic the BBB in vitro, with partial performance can be simulated. The tight junction (TJ) between brain microvascular endothelial cells is responsible to maintain the structure and integrity of BBB, which can be reflected by the resistance value measurement (TEER) in vitro [9, 12-14]. During JEV infection, the highly induced number of proinflammatory cytokines and chemokines contribute to pathogenesis [8]. Increasing evidence suggests that the transmigration of leukocytes from peripheral bloodstream to CNS dependents on the chemokines, which plays a critical role in recruiting leukocytes to CNS in viral encephalitis or non-viral encephalitis [15-18]. Besides, the interactions between cell adhesion molecules and their ligands are involved in immune cells trafficking which is confirmed in the model of gene deficiency animal or specific blockage of those molecules such as ICAM-1, VCAM-1, LFA-1, VLA-4 and E-selectin [12, 17, 19]. The upregulation of VLA-4 and LFA-1, as well as their ligands VCAM-1 and ICAM-1 also enhance immune cells transmigration to the CNS in virus-induced encephalitis [3, 18, 20, 21].

There are several possible routes for flaviviruses invading into the CNS: the infection of brain microvascular endothelium, the spread from the olfactory bulb, and the immune cells acting as “Trojan Horse” [7, 19, 22]. Increasing evidence suggested that the ZIKA virus may cross the BBB without any fluctuation to the integrity of tight junction [11, 23, 24]. It was recently demonstrated that monocytes had been linked with the transmission and pathogenesis of ZIKV [24, 25]. The infiltration of leukocytes into the site of neuroinflammation presents paradoxical characters in the different disease models. The appearance of infected monocyte in the CNS is a signal of carrying virus to the CNS; however, it may also participate in viral clearance in some cases. Nonetheless, the appearance of infected monocyte might be thought of as an indicator of the severity of CNS disease [6, 17, 26, 27]. In HIV infection, the infiltration of HIV-infected T cells or monocytes/macrophages implies the occurrence of CNS invasion, which caused HIV-associated dementia (HAD) [7, 13]. During WNV and TMEV (Theiler's mouse encephalomyelitis virus infection, it is found that the transmigration monocytes can reduce mortality and morbidity [17, 28, 29]. It is also suggested that monocytes facilitate the transmigration of T cells to CNS [18, 30]. Evidence suggested that HIV-1, WNV and ZIKV may spread to the CNS by infiltrated monocytes/T cells via “Trojan horse” pathway, and the accumulation of virus-infected leukocytes may exacerbate the encephalitis [6, 7, 31, 32]. Whether the “Trojan horse” pathway is involved in the JEV neuroinvasion remains elusive.

HMGB1 (high-mobility group box 1), a most well-studied HMG protein, expresses within the nucleus in normal cells, stabilizing the nucleosome structure and inducing DNA bending to regulate transcription as a DNA chaperone [33-35]. HMGB1 can be actively translocated and released from multiple cells responding to the specific stimuli [36, 37]. HMGB1 actively participates in cell recruitment and migration, immune response, microvascular rolling and adhesion, tissue regeneration and invasion, and also acts as a damage-associated molecular pattern (DAMP) with adhesion molecular and chemokine activities [36,

38-43]. Evidence has shown the contribution of extracellular HMGB1 in the migration of numerous cell types including stem cells, endothelial cells, monocytes and dendritic cells [38, 40, 41, 44, 45]. Furthermore, extracellular HMGB1 induces the activation of immune cells and the production of multiple inflammatory factors such as TNF-α, IL-6, and IL-1β [37, 39, 46-49], which may contribute to the disruption of the BBB. In vitro study revealed that HMGB1 is associated with BBB breakdown [50], facilitating immune cells transmigration across the BBB into the brain. Correctly, HMGB1 receptor RAGE (receptor for advanced glycation end-products), a high-affinity receptor of HMGB1, plays a restrictive and essential role during the transendothelial migration of immune cells [38]. Therefore, it is essential to determine the role of HMGB1 in immune cells across the BBB into the CNS during JEV infection.

Until now, the pathways of JEV neuroinvasion are not completely clarified, and this investigation provides evidence of the JEV neuroinvasion pathway. However, there are limited studies on HMGB1 mediating transendothelial migration of monocyte, which expands JEV infection in CNS. JEV-infected monocytes transmit JEV into the CNS suggested that the “Trojan horse” pathway may be employed in JEV invasion which was facilitated by the HMGB1. These data provide insights into the mechanisms of JEV invasion into the CNS and assisted the JE treatment.

Materials And Methods

Mice and virus

C57BL/6 mice were supplied by the Laboratory Animal Center of Huazhong Agricultural University, Wuhan, China. All work obeyed the Committee for Protection, supervision, and the Control of Experiments on Animals guidelines of Huazhong Agricultural University. JEV-P3 strain was employed in our previous research [8] and 15 μl (5×10^4 PFU) of the viral inoculum was injected into the brain of 1-day suckling mice. After euthanizing mice, brains were removed. Homogenized brains were suspended in Dulbecco modified eagle medium (DMEM) forming of 10% (wt/vol). After centrifugation, the debris was discarded and the supernatant was stored at -80°C until use. Baby hamster kidney fibroblast cell line (BHK-21) was used for viral titration by plaque assay.

Virus infection

Female C57BL/6 mice aged 6-8 weeks were classified into two groups: the control group, which was injected with 50 μl volumes of DMEM. And the JEV infected group, mice were injected in the footpad with a volume of 50 μl that contains 10^5 PFU. Control and JEV-infected mice group was maintained for 10 days with tissue sectioning and protein/RNA extraction.

Mice splenocytes and BEMCs (HBMECs, bEnd.3 cells) were exposed to JEV at MOI of 1 and incubated in DMEM at 37°C with 5% CO_2 for 2 h. Washed by PBS, then grown in a maintenance medium. JEV-free cells were serving as a control.

Cell culture and co-culture

HBMECs (Human Brain Microvascular Endothelial Cells) were kept in our laboratory, which was grown in DMEM medium including 10% FBS (fetal bovine serum, Gibco, Grand Island, NY) and endothelial cell growth supplement nonessential amino acids (NEAA), minimum essential medium (MEM) vitamins, sodium pyruvate，100 U/ml penicillin and 100 mg/ml streptomycin sulfate at 37°C with 5% CO_2. BHK-21 cells and bEnd.3 cells were kept in our laboratory, which was grown in DMEM medium including 10% FBS (fetal bovine serum, Gibco, Grand Island, NY), 100 U/ml penicillin and 100 mg/ml streptomycin sulfate at 37°C with 5% CO_2. C6/36 cells were obtained from the Institute of Virology, Chinese Academy of Sciences, cultured at 28°C with 5% CO_2, and the culture medium was consistent with BHK-21 cells.

Primary splenocytes were collected from healthy adult mice. After spinning down the red blood cells, then cultured at a density of 1×10^6 cells/ml in DMEM medium including 10% FBS, 100 U/ml penicillin and 100 mg/ml streptomycin sulfate, splenocytes were treated with recombinant HMGB1 (100 ng/ml) or infected with JEV(MOI=1). Then co-cultured with the JEV-infected BMECs monolayer in the 12-well plate for real-time PCR and immunofluorescence. JEV-free or HMGB1-free cells were serving as a control.

Preparation of the sHMGB1 and rHMGB1

PCDH-CMV plasmid was used for the overexpression of HMGB1 (NM_001313893.1) of 293 T cells, with the paired primer: forward primer: 5’-CCGGAATTCGCCACCAA

CTAAACATGGGCAAAGGAG-3’ and reverse primer: 5’-AAATATGCGGCCGCCA

CCAGGACAGGGCTATCTAA-3’. Cell culture supernatant detection suggested that there was high concertation of supernatant HMGB1(sHMGB1) at 48 h. Recombinant HMGB1 (rHMGB1) was obtained from Sino Biological, China (cat: 10326-H08H).

Western Blotting

Cells were lysed in RIPA buffer including the protease inhibitor cocktail, homogenized, and centrifuged at 12, 000 × g and 4°C for 5 min. Protein concentration was monitored by the BCA protein assay kit (Beyotime, China). Protein samples were isolated by performing SDS-PAGE using 12% polyacrylamide gel electrophoresis. Proteins were transferred to polyvinylidene difluoride membranes (Bio-Rad, Richmond, CA, USA). Then blocked for 2 h at room temperature in Tris-buffered saline with Tween 20 (TBST) containing 5% nonfat dry milk, after incubated with JEV-E protein (preserved in the laboratory previously) monoclonal antibody, ICAM-2, beta-catenin, E-Selectin (Proteintech, China), HMGB1 (Novus Biotechnology, NA, USA) and VE-Cadherin, VCAM-1 (Abcam, USA) overnight at 4°C. Washed by TBST, then incubated members with horseradish peroxidase-conjugated (HRP) antibodies. Enhanced chemiluminescence reagents (Bio-Rad, Richmond, CA, USA) was utilized to develop the HRP. All the data are presented as the means ± SEMs (the standard errors of the mean).

Immune cellsbrain injection

Incubated JEV-infected $CD3^+$ T cells, $CD19^+$ B cells and $Ly6C^+$ monocytes with the JEV antiserum, and injected into normal mice brain. JE onset time data were registered, and the JE mice brain was removed for virus detection.

Immunohistochemical and Immunofluorescence (IF)

Ketamine-xylazine (0.01 ml/g) and PBS were used for the anesthetization and perfusion of the symptomatic mice. Immediately the collected brains, olfactory bulbs and spinal cords were fixed with 4% paraformaldehyde in an aseptic environment. All the fixed tissues were embedded by paraffin for sections. And the antigen was repaired in 0.01 M sodium citrate solution buffer thermally.

Tissues sections were blocked in 5% BSA sealing fluid for 30 min at room temperature and incubated with JEV-E protein monoclonal antibody overnight at 4℃. Washed by PBS, incubated with the second antibody for 1 h, and nuclear stained with DAPI for 3 min at room temperature. The tissue sections were sealed with glycerin. The fluorescence microscope was used for the observation of the sealing section.

BBBmonolayer transwell model

The BBB monolayer transwell model (Corning, USA) was adopted in this study. 200 μl (50 μg/ml) rat tail collagen (Sigma, USA) was used to enclose an upper chamber at room temperature for 1 h. After washing, 500 μl DMEM (no phenol red, Sigma, USA) was used for the upper chamber pre-equilibration at 37°C for 1 h. BMEC (HBMECs, bEnd.3 cells) were cultured in the upper chamber with a total volume of 500 μl culture medium (no phenol red, Sigma, USA) at 37°C, 5% CO_2 for about 24 h. The leakage examination was continued for 4 h, and 10 kD and 70 kD FITC-dextran (Sigma-Aldrich, USA) and employed for the permeability measurement of the BBB monolayer model. TEER (transendothelial electrical resistance) (Millipore, Billerica, MA) belonging to the evaluation criteria of the monolayer models in vitro, which were monitored and recorded at indicated times (0 h, 6 h, 12 h, 18 h, 24 h).

Immune cells transmigration

Splenocytes were provided from three individual mice at least. 500 μL (5×10^5) cells were added into the upper chamber (PC file) of the transwell model (Corning, USA), which were already fully covered with JEV-infected BMEC (HBMEC or bEnd.3 cell) and passed permeability detection. After co-cultured for 24 hours, transmigrated immune cells were collected from the lower chamber, and stained by fluorescence antibody labelling for the detection of flow cytometry.

Flow Cytometry and Quantitative real-time PCR analysis

Suspension of splenocytes was stained with the combination of mAbs conjugated with FITC, PE, PE-Cy7, APC-Cy7, PB and APC. For the cell surface marker staining, spleen cells suspensions were incubated with the subjacent Abs: CD3, CD11b, Ly6C, CD19 in PBS buffer (pH=7.4) containing 0.2% BSA (BioSharp, USA) at 4°C for 30 min. PBS was provided for double washing (400×g, 5 min, 4°C), and cell suspension. Cells determination and separation were achieved by FACS Calibur (BD Biosciences, USA) system Beckman

cytoFlex (Beckman Coulter, USA) and CytExport 2.0 CellQuest Pro software were for data analyzing. The utilizing of EGFP-JEV has a critical contribution to intracellular JEV detection.

Total RNA was extracted with TRIZOL reagent (Invitrogen, Grand Island, NY, USA). 1 μg RNA served to synthesize cDNA using ReverTra Ace RT-PCR RT kit (Toyobo, Japan), followed the manufacturer's instructions. SYBR green (Invitrogen, Grand Island, NY, USA) was employed to quantitative real-time PCR using the StepOne Plus binding StepOne Software v2.2.2 (Applied Biosystems, Foster City, CA, USA). The relative expression of the JEV-C gene in the spleen or brain was normalized to the level of control β-actin. The pcDNA3.0-HA/JEV-C gene plasmid was served as a template for generating a standard curve to quantify the copy numbers of JEV. Following real-time PCR primers were list in supplementary Table 1.

Statistical analysis.

All experiments currently were repeated for several times. Fig. 9 was made on the website of https://app.biorender.com/. Data were expressed as the means ± SEMs, and the significance of differences between groups was followed by Tukey's post hoc tests. Graphs were plotted and analyzed using GraphPad Prism (v7.0; GraphPad, La Jolla, CA, USA).

Results

JEV infection induced the translocation and secretion of HMGB1 in HBMEC

The HBMECs were infected with JEV at 1 MOI, and the expression of JEV-E protein was measured by Western blotting. JEV replicates in HBMEC in a time-dependent manner (Fig. 1A), abundant JEV-E protein presented intracellularly at 24 h and 48 h (Fig. 1B). JEV-infection induced a dramatical increase of HMGB1 both in mRNA (Fig. 1C), and protein level (Fig. 1D). Meanwhile, HMGB1 was also highly expressed in mouse brain microvascular endothelial cell line bEnd.3 during JEV infection (S.1). These results demonstrate that brain microvascular endothelial cells are susceptible to JEV that particularly induces HMGB1 production in brain microvascular endothelial cells.

The biological functions of HMGB1 are dominated by its expression and subcellular location [51]. Thus, the HMGB1 intracellular distribution and release after JEV infection on HBMEC was determined. HMGB1 was predominantly located in the nucleus of uninfected cells at a low level detected by confocal immunofluorescence microscopy (Fig. 1E). At 6 h, 12 h and 24 h, there was a significant increase of HMGB1 at the cytoplasm in HBMEC, which suggested the translocation of HMGB1 from the nucleus to the cytoplasm (Fig. 1E). To further confirm this phenomenon, the protein was extracted from the different cell compartment, the nuclear and the cytoplasmic. And then, the expression of HMGB1 was measured with JEV infection at 1 MOI. The results showed a significant increase of HMGB1 in the cytoplasm after JEV infection, and reached a peak at 12 h, and then gradually slowed-down from 24 h to 48 h. The expression of HMGB1 in the nucleus concomitantly increased at 6 h and slipped to the lower level from 12 h to 48 h after JEV infection (Fig. 1F). It further confirmed that JEV-infection stimulated the cellular expression of HMGB1, and HMGB1 translocated from the nucleus to the cytoplasm. The accumulation of

HMGB1 in the cytoplasm could actively trigger the autocrine, which is governed by post-translational modifications. Brefeldin A, an inhibitor of intracellular protein transport, was applied to HBMEC after 12 h postinfection. The intracellular distribution of HMGB1 was observed by the confocal laser scanning microscope. Inhibition of vesicles by Brefeldin A dramatically suppressed HMGB1 release accompanied with an increase of the cytoplasmic HMGB1 at 24 h (Fig. 1G), which suggested that the increased intracellular expression of HMGB1 could be released to the extracellular space.

Taken together, these data suggested that JEV induced HMGB1 upregulation and translocation from the nucleus to the cytoplasm in brain microvascular endothelial cells, and then subsequently released from the cells.

JEV infection induced activation of BMECs and increased adhesion molecules

Brain microvascular endothelial cells are critical in forming BBB and maintaining the barrier function. High expression of adhesion molecules and integrin ligands is necessary for immune cells adhesion to BBB endothelium, which facilitates the immune cell infiltration into the CNS. To identify the underlying mechanism of leukocytes crossing BBB, yeast cells which highly express GFP-LFA-1 (ICAM-1 ligand) were used to detect the interaction with JEV-activated endothelial cells [52]. It was found that more GFP-LFA-1 yeast cells were attached to JEV-infected bEnd.3 monolayer than control cells (Fig. 2A, B), which suggested that JEV caused an upregulation of ICAM-1 on bEnd.3 monolayer. Western blotting also confirmed the upregulation of adhesion molecules on endothelial cells after JEV infection, including VCAM-1, ICAM-2, E-Selectin, VE-Cadherin and beta-catenin (Fig. 2C, D). As expected, recombinant HMGB1(100 ng/ml) induced upregulation of LFA-1 and VLA-4 on mice splenocytes, which act as the receptor of ICAM-1 and VCAM-1 (Fig. 2E, F). Furthermore, we found an upregulation of ICAM-1 and VCAM-1 in the brain, and a corresponding increase of LFA-1 and VLA-4 in the spleen of the JEV-infected mouse model (S. 3A, B, C, D).

Meanwhile, the expression of adhesion molecules on HBMEC was determined with real-time PCR, which showed an increase of ICAM-1, VCAM-1 after JEV infection (S. 2A, B). With the treatment of recombinant HMGB1, an upregulation was also observed in the expression of LFA-1 (CD11a and CD18) and VLA-4 (CD49d and CD29) on human THP-1 cells (S. 2C, D).

All these results suggested that JEV infection induced the upregulation of adhesion molecules on BMEC, and HMGB1 also increased the integrin ligands of immune cells during early JEV infection, which could facilitate the interaction between immune cells and the BBB endothelium.

Extracellular HMGB1 promoted immune cells adhesion to endothelium

Leukocyte-endothelium adhesion is indispensable for immune cell CNS infiltration. 293 T cells were used to overexpress HMGB1, and the supernatant was collected to treat the THP-1 cells. The results showed an increase of THP-1 cell adhesion to JEV-infected HBMEC monolayer with the treatment of supernatant containing HMGB1 (Fig. 3A). Trichostatin A (TSA), a deacetylase inhibitor, have been shown to stimulate

the hyperacetylation of HMGB1 as well as histones which facilitates the release of HMGB1 from chromatin. Besides, the secreted HMGB1 (sHMGB1) dramatically increased THP-1 cells adhering to the JEV-activated HBMEC monolayer than that of the uninfected group in vitro (Fig. 3A). Moreover, the adhesion was measured between GFP^+-leukocytes from JEV-infected mice and bEnd.3 cell preincubated with JEV-P3 virus. More GFP^+ cells were found adhering on bEnd.3 cells primed with alive JEV-P3 virus, but not found on the cells treated with UV-deactivated virus (Fig. 3B). To further study the function of HMGB1, mouse splenocytes were treated with recombinant HMGB1 (rHMGB1), and co-cultured with bEnd.3 monolayers. It was found that rHMGB1 increased the adhesion of $Ly6C^+CD11b^+$ monocytes to the JEV-primed bEnd.3 monolayer (Fig. 3C, D). However, there was no significant change of the HMGB1-treated adhering $CD3^+$ T cells and $CD19^+$ B cells to the JEV-primed endothelial monolayer (Fig. 3C, D). Furthermore, JEV infection enhanced the purified $Ly6C^+$ monocyte adhesion to the BMEC monolayer in vitro (Fig. 3E). These results indicated that JEV-activated endothelium promoted the adhesion of immune cells and the presentation of extracellular HMGB1 enhanced monocytes adhering to BMEC monolayer, which may potentiate immune cells crossing BBB entry into the CNS.

Furthermore, a rearrangement in F-actin in BMECs was noticed F-actin in BMEC in the early stage of JEV-infection, while no significant change was found with the treatment of UV-inactivated JEV-P3 (UV-P3) (S. 4A). Notably, there was no significant effect on the endothelium integrity with JEV-treatment in vitro; with no difference between the live virus or UV-inactivated virus (S. 4B). However, JEV-infected mouse brain supernatant (10□) caused fluctuation to endothelial cells integrity in vitro with the dramatic decrease of RB value (from 15 to 50 h) of BMEC monolayer (S. 4B), which suggested that JEV per se does not disrupt the BBB. However, JEV infection induced the inflammatory responses to break down the BBB.

Extracellular HMGB1 facilitated transendothelial migration of JEV-infected monocytes

Data above suggested that the presence of HMGB1 increased the transmigration of THP-1 cells in the JEV-infected monolayer model. To emphasize, the BMEC monolayer was employed to elucidate the role of extracellular HMGB1 in leucocytes migration during JEV infection. We used 10 kD and 70 kD dextrans to visualize the spatially variable, size-dependent permeability of the monolayer (Fig. 4A). Without JEV stimulation, the TEER value, which reflects the integrity of the BBB, were kept stable over 24 hours (>200 $\Omega \times cm^2$), which implied the integrity of the BBB monolayer in vitro (Fig. 4B). Accompanied with the decrease of TEERs, more $Ly6C^+CD11b^+$ monocytes, $CD3^+$ T cells, and $CD19^+$ B cells transmigrated from the upper chamber to the lower chamber in the JEV-infected monolayer models (Fig. 4B, C, D). A high concentration of rHMGB1 exacerbated the destruction of the monolayer models during the early infection (Fig. 4B). Moreover, rHMGB1 increased mice $Ly6C^+CD11b^+$ monocytes transmigrating from the upper chamber to the lower chamber, while there was no significant change of $CD3^+$ T cells, and $CD19^+$ B cells compared to JEV-infected group (Fig. 4B, C, D). These results indicated that JEV infection caused BBB fluctuation and increased immune cell CNS infiltration during early infection, which was aggravated by HMGB1. Furthermore, infection-induced HMGB1 enhanced monocyte transendothelial migration, which was based on leukocyte-endothelium adhesion, resulting in BBB breakdown during early infection.

To discover whether transmigrated immune cells act as virus carriers, JEV with EGFP tag (EGFP-JEV) was applied to the bEnd.3 monolayer to visualize the transmigration of immune cells (Fig. 5A). On the contrary, during JEV infection, the TEER value decreased with time, which means that the integrity of the monolayer was compromised, and the permeability accordingly increased (Fig. 5B). More importantly, the decrease of TEER coincided with an increased number of immune cells transmigrating into the lower chamber. The migrated cells, including $Ly6C^+CD11b^+$ monocytes, $CD3^+$ T cells and $CD19^+$ B cells, were measured in the absence or presence of the virus. The migratory capability was enhanced in the presence of EGFP-JEV (Fig. 5E). In addition, more $EGFP^+Ly6C^+CD11b^+$ monocytes infected transmigrated from the upper chamber to the lower chamber than $CD3^+$ T cells with EGFP-JEV infection, and only a few transmigrated $CD19^+$ B cells were detected in the lower chamber (Fig. 5F). These results showed that the disruption of the BBB monolayer model increases transmigration of immune cells, especially $Ly6C^+CD11b^+$ monocytes after JEV infection.

These data suggested that extracellular HMGB1 promotes the leukocytes transendothelial migration, especially for monocyte during early infection. Meanwhile, the infected monocytes, T cells and B cells carried JEV participating in transendothelial migration, which acts as “Trojan horse”, may enhance JEV neuroinvasion and aggravate JE.

Transmigration of JEV-infected immune cells correlated with the onset of JE in mice

The correlation between JEV-infected transmigrated splenocytes and the JE incidence in vivo needs further confirmation. Hence, $Ly6C^+$ monocytes, $CD3^+$ T cells and $CD19^+$ B cells were purified by flow cytometry, which were exposed with JEV at MOI of 1. There was a high replication of JEV in splenocytes at 24 h (Fig. 6A). Western blot demonstrated that there was inclusive JEV inside the isolated splenocytes (Fig. 6B). Then, these cells were incubated with the anti-JEV serum to neutralize the non-specific adhesive viruses and injected into the brain of healthy adult mice at 1×10^5 cells respectively. Furthermore, the initial onset of JE was much earlier in the intracranial injection of JEV-infected $Ly6C^+$ monocyte and $CD3^+$ T cells than the injection of JEV-infected $CD19^+$ B cells (Fig. 6C). No doubt, all the mice delivered JEV-infected immune cells resulted in JE ultimately, which were further supported by the detection of JEV in the brain by immunofluorescence (Fig. 6D, E, F). Moreover, there was a positive association between the onset time of JE and the quantity of transformed JEV-infected immune cells. These data indicated that the transmigration of JEV-infected immune cells from the circulation to the brain were precisely associated with JE onset in the early stage.

The natural infection route was also mimicked by JEV footpad injection in C57BL/6 mice. Tissue samples were collected from the cerebrum, olfactory bulb and spinal cord after infection, and the viral loads were determined by real-time PCR. The results showed that JEV tends to accumulate early in the cerebrum than that of olfactory bulbs and spinal cords (S. 6A, B), suggesting that the hematogenous route, rather than the olfactory nerve or long-range retrograde axonal transport, is more feasible in the JEV neuroinvasion. To further confirm that the hematogenous route is one of those pathways for JEV

spreading into the CNS; Immunofluorescence was conducted to determine the JEV distribution in the different neuronal tissues, including the cerebrum, olfactory bulb, and spinal cord. A high count of the JEV virus existed in cerebrum in comparison, to the fewer count entered the CNS via the olfactory bulb or retrograded axonal transportation (S. 6D). These results demonstrated that cerebrum was the primary target of the JEV and the hematogenous route was one of the major pathways in the JEV neuroinvasion.

Together, these data indicated that the hematogenous pathway could be utilized by JEV, while the transmigration of JEV-infected monocytes, T cells and B cells were relevant to the onset of JE in mice.

Discussion

HMGB1 (amphoterin) is a DNA-binding, intracellular transcription regulation protein [36]. Cell activation or necrosis induces HMGB1 translocating to the cytoplasm and releasing to the extracellular space [37]. Extracellular HMGB1 has been described as a DAMP mediating the inflammatory responses and regarded as a cell migration mediator [36, 40, 41, 53]. In this study, we demonstrated that BMEC-derived HMGB1 promoted the infiltration of immune cells in vitro. That was performed by the enhancement of leukocyte-endothelium adhesion and the increase of transmigration immune cells. Altogether, this evidence indicated that HMGB1, as a critical adhesion and cell transendothelial migration mediator, was involved in the “Trojan horse” pathway in JEV neuroinvasion, contributing to BBB breakdown and JEV pathogenesis.

Previous studies have reported that RSV, H5N1, WNV, DENV, and HIV-1 induced HMGB1 production and release, which played a significant mediator role of inflammation during these viral infections [37, 54]. Also, HMGB1 is an essential cytokine in cell migration, especially in monocyte transendothelial migration [36, 38]. This investigation initially illustrated that JEV infection induced the HMGB1 release from intracellular to extracellular in the HBMEC. The appearance of intracellular vesicles inhibitor caused an increase of cytoplasmic HMGB1. Therefore, although HMGB1 belongs to classical leader peptide lacking protein, the translocation and extracellular release of HMGB1 may be via the nonclassical vesicle-dependent secretory manner in BEMC [42, 55]. Moreover, studies have found that classical protein kinase C phosphorylation and calcium/calmodulin-dependent kinases are also included in HMGB1 secretion [56, 57].

Our results showed that JEV infection also indicated a cytoskeletal rearrangement in endothelial cells, and previous studies have shown that JEV infection caused the release of inflammatory factors, which were described as a sign for endothelial cell activation [12]. Furthermore, the activated endothelial cells upregulated the expression of adhesion-related molecules, such as ICAM-1, VCAM-1, and increased the level of LFA-1 and VLA-4 in vivo and in vitro during infection. It was also found that rHMGB1 upregulated the expression of LFA-1 and VLA-4 both in THP-1 cells and in mouse splenocytes in vitro. More evidence presented that the interaction of adhesion molecules and integrin ligands facilitate the transmigration of adhesion immune cells [11, 19-21, 32], which accounts for the increase of adhesion immune cells to the BMECs monolayer during early infection. These results indicated that BMEC-derived HMGB1 mediated

immune cells adhering to the BBB in a coordinated manner with the increase of adhesion-associated molecules, which might enhance leukocyte transendothelial migration across the BBB, promoting JEV-infected immune cells brain invasion.

Beside adhesion molecules and ligands, we also found that HMGB1 played an important role in leukocyte migration across the BBB during early infection. Interactions between HMGB1 and cell surface receptors participate in the migration of various kinds of cells such as dendritic cell, tumor cell, endothelial cell, neutrophil and monocyte [36, 38, 58]. Most invading pathogens induced the high expression of inflammatory cytokines and chemokines and caused inflammatory responses, leading to degradation of tight junction proteins and disruption of the BBB, uncontrolled transmigration of leukocytes into the CNS, and ultimately causing neuronal damage of the CNS [7, 10, 12, 59, 60]. At the same time, virus infection upregulated the levels of chemokines such as CCL5, CCL2, which plays an essential role in the recruitment of immune cells [3]. Nonetheless, we focused on the HMGB1-mediated transendothelial migration of monocytes entry into CNS during infection. Our previous results revealed that JEV itself caused no significant damage to the tight junctions of endothelial cells during early infection, which was different to other neurotropic Flaviviridae such as WNV [6, 61, 62]. On the contrary, the JEV-infected brain supernatant containing MMPs, IL-6, TNF-□, CCL-2 and other soluble pro-inflammatory factors, dramatically destroyed the integrity of endothelial cells monolayer in vitro, supporting that the systemic inflammatory response breakdown the BBB during early infection [8, 11, 63].

Endothelial cells, coupled with pericytes, glia, and neurons constitute a relatively moderate physiological barrier to determine transportation of the CNS and maintain a relatively balanced physiological state, which is considered to form the BBB [6, 7, 10]. HMGB1 mediates monocyte transendothelial migration, which was already adhered to the endothelium, collaborative with the JEV-activated endothelium, enhancing leukocytes adhesion and inflammatory responses, subsequently leading the fluctuation of the BBB, promoting monocyte infiltration. It has shown that during HIV/WNV infection, immune cells (monocytes, T cells) act as the virus carriers were also recruited to the BBB surface for CNS infiltration [7, 17, 28]. Our results revealed that HMGB1 mediated monocyte transendothelial migration into the CNS during JEV infection. It was demonstrated that JEV induced significant fluctuation to the endothelial barrier in co-culture models, while not in the monoculture BBB models. Extracellular HMGB1 also activates immune cells to produce inflammatory cytokines [49]. HMGB1 enhances inflammatory response and leukocyte-endothelium adhesion when destroying the BBB, which was reflected by the decrease of TEERs and the increase of migration cells during early infection. Moreover, evidence showed that HMGB1 was directly related to the breakdown of the BBB in vitro [50]. However, neither the BBB monolayer model nor the in vitro transwell model can fully represent the intact BBB in vivo [64]. More comprehensive BBB models in vivo or in vitro are being developed or sought for the investigation of HMGB1-mediated JEV-infected monocytes in the early stage of viral neuroinvasion. The migration of immune cells is probably different in monocytes and T cells in response to HMGB1, which may explicate the distinction in transmigration efficiency in our model. Furthermore, our data suggested that HMGB1 is concerned with the breakdown of the BBB and immune cells infiltration into the CNS during JEV infection. All the results suggested that BMEC-derived HMGB1 facilitated the endothelium adhesion and

transendothelial migration of monocytes during JEV infection. JEV-infected monocyte mingled with a few of other leukocytes acts as the “Trojan horse”, transporting virus into the CNS, resulted in JEV neuroinvasion.

To determine whether transmigrated JEV-infected immune cells induce JE, JEV-carrying immune cells were injected into the brain of healthy adult mice. Not surprisingly, JEV-infected monocytes invaded into the CNS, leading to the advanced onset of JE, expanding virus infection in the brain. The presence of monocytes in the brain is a characteristic feather of the CNS inflammation in viral encephalitis, which contributes to reducing viral burden generally [17]. Paradoxically, studies have shown that monocytes were capable of infiltrating into the CNS during viral encephalitis, and of differentiating into a certain type of macrophage, upregulating the production of proinflammatory cytokines, such as NO, MMP and other molecules. Activated immune cells were involved in the inflammatory response, contributing to the BBB breakdown and CNS tissue damage and eventually long-term neurological sequelae or mortality [3, 7, 8, 11, 30]. The intracranial injection of JEV-infected T cells initially caused the occurrence of JE. Notably, the appearance of T cells in CNS was possibly regulated by the transmigration of monocytes [30, 65, 66]. Although evidence revealed that inverse neural pathway is also employed in JEV neuroinvasion [67], neurotropic viruses might spread via multiple pathways to achieve the CNS invasion [19]. Our results suggested that CNS invading immune cells such as JEV-carried monocytes and T cells, caused the occurrence of obvious clinical symptoms of JE early, which was contributed by BMEC-derived HMGB1 during the early stage of JEV infection.

Viruses invasion led to the release of HMGB1, which may play a critical chemotactic role during the early stage. BMEC-derived HMGB1 caused integrins to increase on immune cells, enhancing immune cell adhesion to the BBB and transendothelial migration, contributing to viral spread and inflammation. Studies have reported that ds-HMGB1 triggers inflammatory response may be involved in the development of JE. There is no doubt that other cells or cytokines were involved in JEV neuroinvasion in vivo. We also discovered that JEV tends to accumulate in the cerebral cortex easily during JEV infection in mice. Hence, we discovered that the hematogenous pathway might be involved in the JEV neuroinvasion and the “Trojan horse” pathway. It is possibly expanding the infection of JEV in CNS accelerating the disease, leading to serious encephalitis, whose emergence is inseparable for the monocyte transmigration.

In summary, our results provide evidence that HMGB1 promotes the peripheral monocytes carrying the JEV to sneak into the CNS as “Trojan horse” (Fig. 7). JEV infection induced the release of HMGB1 from brain microcircuit endothelial cells, which stimulates adhesion molecules upregulation on BBB-endothelial cells, and corresponding ligands upregulation on monocytes. Thus, the interaction between monocytes and BBB-endothelial cells is enhanced. As a consequence, JEV-infected monocytes transmigrate more frequently from the peripheral to the CNS, leading to neuroinfection and neuroinflammation.

Conclusion

This investigation presents evidence that the JEV-infected immune cells which act as the “Trojan horse” are involved in JEV brain invasion. JEV infection induced the release of HMGB1 from brain microcircuit endothelial cells and, contributed to the infiltration of JEV-infected monocytes into the CNS, accelerating the onset of JE. Therefore, JEV-infected monocytes CNS migration and extracellular HMGB1 can be discussed as the therapeutic target of JE treatment.

Abbreviations

BBB: Blood-brain barrier

BMEC: Brain microvascular endothelial cell

CNS: Central nervous system

ICAM-1: Intercellular adhesion molecule 1

ICAM-2: Intercellular adhesion molecule 2

JE: Japanese encephalitis

JEV: Japanese encephalitis virus

HBMEC: Human brain microvascular endothelial cell

HMGB1: High Mobility Group Box 1

LFA-1: Lymphocyte function-associated antigen 1

rHMGB1: recombinant HMGB1

TEER: Transendothelial electrical resistance

VLA-4: Very Late Antigen 4

VCAM-1: Vascular cell adhesion molecule 1

Declarations

Acknowledgements

The authors thank Dr Bo Zhang (Wuhan Institute of viruses, Chinese Academy of Science, China) for permission to employ the EGFP-JEV.

Funding

This work was support by the financial support provided by the National Program on Key Research Project of China (2016YFD0500406), the Fundamental Research Fund for the Central University, and the funds of the State Key Laboratory of Agricultural Microbiology.

Authors' contributions

MC and SSZ designed the investigation; SSZ, NYC, QCZ and WJX performed the experiments；SSZ, WJX, KW and NYC analyzed the data; MC and SSZ organized the data; SSZ and MC wrote the paper. All authors read and agreed to the final manuscript.

Ethics approval and consent to participate

All animal experiments were conducted by experimental protocols (number: Hzaumo-2015-018) were approved by the Research Ethics Committee of the College of Veterinary Medicine, Huazhong Agricultural University, Hubei, Wuhan, China.

Consent for publication

Not applicable.

Availability of data and material

All data supporting the conclusions are included in the article.

Competing interests

The authors declare that they have no competing interests.

References

1. Misra UK, Kalita J: **Overview: Japanese encephalitis.** *Prog Neurobiol* 2010, **91:**108-120.
2. Solomon T, Dung NM, Kneen R, Gainsborough M, Vaughn DW, Khanh VT: **Japanese encephalitis.** *J Neurol Neurosurg Psychiatry* 2000, **68:**405-415.
3. Lannes N, Summerfield A, Filgueira L: **Regulation of inflammation in Japanese encephalitis.** *J Neuroinflammation* 2017, **14:**158.
4. Turtle L, Solomon T: **Japanese encephalitis - the prospects for new treatments.** *Nat Rev Neurol* 2018, **14:**298-313.
5. Wang G, Li H, Yang X, Guo T, Wang L, Zhao Z, Sun H, Hou X, Ding X, Dou C, et al: **Guillain-Barre Syndrome Associated with JEV Infection.** *N Engl J Med* 2020, **383:**1188-1190.
6. Spindler KR, Hsu TH: **Viral disruption of the blood-brain barrier.** *Trends Microbiol* 2012, **20:**282-290.
7. Koyuncu OO, Hogue IB, Enquist LW: **Virus infections in the nervous system.** *Cell Host Microbe* 2013, **13:**379-393.

8. Li F, Wang Y, Yu L, Cao S, Wang K, Yuan J, Wang C, Cui M, Fu ZF: **Viral Infection of the Central Nervous System and Neuroinflammation Precede Blood-Brain Barrier Disruption during Japanese Encephalitis Virus Infection.** *J Virol* 2015, **89:**5602-5614.
9. Hsieh JT, Rathore APS, Soundarajan G, St John AL: **Japanese encephalitis virus neuropenetrance is driven by mast cell chymase.** *Nat Commun* 2019, **10:**706.
10. Obermeier B, Daneman R, Ransohoff RM: **Development, maintenance and disruption of the blood-brain barrier.** *Nat Med* 2013, **19:**1584-1596.
11. Mustafa YM, Meuren LM, Coelho SVA, de Arruda LB: **Pathways Exploited by Flaviviruses to Counteract the Blood-Brain Barrier and Invade the Central Nervous System.** *Front Microbiol* 2019, **10:**525.
12. Varatharaj A, Galea I: **The blood-brain barrier in systemic inflammation.** *Brain Behav Immun* 2017, **60:**1-12.
13. Sagar D, Lamontagne A, Foss CA, Khan ZK, Pomper MG, Jain P: **Dendritic cell CNS recruitment correlates with disease severity in EAE via CCL2 chemotaxis at the blood-brain barrier through paracellular transmigration and ERK activation.** *J Neuroinflammation* 2012, **9:**245.
14. Chen CJ, Ou YC, Li JR, Chang CY, Pan HC, Lai CY, Liao SL, Raung SL, Chang CJ: **Infection of pericytes in vitro by Japanese encephalitis virus disrupts the integrity of the endothelial barrier.** *J Virol* 2014, **88:**1150-1161.
15. Lim JK, Obara CJ, Rivollier A, Pletnev AG, Kelsall BL, Murphy PM: **Chemokine receptor Ccr2 is critical for monocyte accumulation and survival in West Nile virus encephalitis.** *J Immunol* 2011, **186:**471-478.
16. Kim JH, Patil AM, Choi JY, Kim SB, Uyangaa E, Hossain FM, Park SY, Lee JH, Kim K, Eo SK: **CCL2, but not its receptor, is essential to restrict immune privileged central nervous system-invasion of Japanese encephalitis virus via regulating accumulation of CD11b(+) Ly-6C(hi) monocytes.** *Immunology* 2016, **149:**186-203.
17. Terry RL, Getts DR, Deffrasnes C, van Vreden C, Campbell IL, King NJ: **Inflammatory monocytes and the pathogenesis of viral encephalitis.** *J Neuroinflammation* 2012, **9:**270.
18. Man S, Ubogu EE, Ransohoff RM: **Inflammatory cell migration into the central nervous system: a few new twists on an old tale.** *Brain Pathol* 2007, **17:**243-250.
19. Miner JJ, Diamond MS: **Mechanisms of restriction of viral neuroinvasion at the blood-brain barrier.** *Curr Opin Immunol* 2016, **38:**18-23.
20. Ley K, Reutershan J: **Leucocyte-endothelial interactions in health and disease.** *Handb Exp Pharmacol* 2006**:**97-133.
21. Lai CY, Ou YC, Chang CY, Pan HC, Chang CJ, Liao SL, Su HL, Chen CJ: **Endothelial Japanese encephalitis virus infection enhances migration and adhesion of leukocytes to brain microvascular endothelia via MEK-dependent expression of ICAM1 and the CINC and RANTES chemokines.** *J Neurochem* 2012, **123:**250-261.

22. Suthar MS, Diamond MS, Gale M, Jr.: **West Nile virus infection and immunity.** *Nat Rev Microbiol* 2013, **11:**115-128.
23. Papa MP, Meuren LM, Coelho SVA, Lucas CGO, Mustafa YM, Lemos Matassoli F, Silveira PP, Frost PS, Pezzuto P, Ribeiro MR, et al: **Zika Virus Infects, Activates, and Crosses Brain Microvascular Endothelial Cells, without Barrier Disruption.** *Front Microbiol* 2017, **8:**2557.
24. Pardigon N: **Pathophysiological mechanisms of Flavivirus infection of the central nervous system.** *Transfus Clin Biol* 2017, **24:**96-100.
25. Bramley JC, Drummond CG, Lennemann NJ, Good CA, Kim KS, Coyne CB: **A Three-Dimensional Cell Culture System To Model RNA Virus Infections at the Blood-Brain Barrier.** *mSphere* 2017, **2**.
26. Charlier C, Nielsen K, Daou S, Brigitte M, Chretien F, Dromer F: **Evidence of a role for monocytes in dissemination and brain invasion by Cryptococcus neoformans.** *Infect Immun* 2009, **77:**120-127.
27. Drevets DA, Dillon MJ, Schawang JE, Stoner JA, Leenen PJ: **IFN-gamma triggers CCR2-independent monocyte entry into the brain during systemic infection by virulent Listeria monocytogenes.** *Brain Behav Immun* 2010, **24:**919-929.
28. Getts DR, Terry RL, Getts MT, Muller M, Rana S, Shrestha B, Radford J, Van Rooijen N, Campbell IL, King NJ: **Ly6c+ "inflammatory monocytes" are microglial precursors recruited in a pathogenic manner in West Nile virus encephalitis.** *J Exp Med* 2008, **205:**2319-2337.
29. Christophi GP, Hudson CA, Panos M, Gruber RC, Massa PT: **Modulation of macrophage infiltration and inflammatory activity by the phosphatase SHP-1 in virus-induced demyelinating disease.** *J Virol* 2009, **83:**522-539.
30. Savarin C, Stohlman SA, Atkinson R, Ransohoff RM, Bergmann CC: **Monocytes regulate T cell migration through the glia limitans during acute viral encephalitis.** *J Virol* 2010, **84:**4878-4888.
31. de Carvalho GC, Borget MY, Bernier S, Garneau D, da Silva Duarte AJ, Dumais N: **RAGE and CCR7 mediate the transmigration of Zika-infected monocytes through the blood-brain barrier.** *Immunobiology* 2019, **224:**792-803.
32. Ayala-Nunez NV, Follain G, Delalande F, Hirschler A, Partiot E, Hale GL, Bollweg BC, Roels J, Chazal M, Bakoa F, et al: **Zika virus enhances monocyte adhesion and transmigration favoring viral dissemination to neural cells.** *Nat Commun* 2019, **10:**4430.
33. Stros M: **HMGB proteins: interactions with DNA and chromatin.** *Biochim Biophys Acta* 2010, **1799:**101-113.
34. Muller S, Scaffidi P, Degryse B, Bonaldi T, Ronfani L, Agresti A, Beltrame M, Bianchi ME: **New EMBO members' review: the double life of HMGB1 chromatin protein: architectural factor and extracellular signal.** *EMBO J* 2001, **20:**4337-4340.
35. Romani M, Rodman TC, Vidali G, Bustin M: **Serological analysis of species specificity in the high mobility group chromosomal proteins.** *J Biol Chem* 1979, **254:**2918-2922.
36. Kang R, Chen R, Zhang Q, Hou W, Wu S, Cao L, Huang J, Yu Y, Fan XG, Yan Z, et al: **HMGB1 in health and disease.** *Mol Aspects Med* 2014, **40:**1-116.

37. Hosakote YM, Brasier AR, Casola A, Garofalo RP, Kurosky A: **Respiratory Syncytial Virus Infection Triggers Epithelial HMGB1 Release as a Damage-Associated Molecular Pattern Promoting a Monocytic Inflammatory Response.** *J Virol* 2016, **90:**9618-9631.
38. Rouhiainen A, Kuja-Panula J, Wilkman E, Pakkanen J, Stenfors J, Tuominen RK, Lepantalo M, Carpen O, Parkkinen J, Rauvala H: **Regulation of monocyte migration by amphoterin (HMGB1).** *Blood* 2004, **104:**1174-1182.
39. Scaffidi P, Misteli T, Bianchi ME: **Release of chromatin protein HMGB1 by necrotic cells triggers inflammation.** *Nature* 2002, **418:**191-195.
40. Furlani D, Donndorf P, Westien I, Ugurlucan M, Pittermann E, Wang W, Li W, Vollmar B, Steinhoff G, Kaminski A, Ma N: **HMGB-1 induces c-kit+ cell microvascular rolling and adhesion via both toll-like receptor-2 and toll-like receptor-4 of endothelial cells.** *J Cell Mol Med* 2012, **16:**1094-1105.
41. Palumbo R, Bianchi ME: **High mobility group box 1 protein, a cue for stem cell recruitment.** *Biochem Pharmacol* 2004, **68:**1165-1170.
42. Degryse B, Bonaldi T, Scaffidi P, Muller S, Resnati M, Sanvito F, Arrigoni G, Bianchi ME: **The high mobility group (HMG) boxes of the nuclear protein HMG1 induce chemotaxis and cytoskeleton reorganization in rat smooth muscle cells.** *J Cell Biol* 2001, **152:**1197-1206.
43. Palumbo R, Sampaolesi M, De Marchis F, Tonlorenzi R, Colombetti S, Mondino A, Cossu G, Bianchi ME: **Extracellular HMGB1, a signal of tissue damage, induces mesoangioblast migration and proliferation.** *J Cell Biol* 2004, **164:**441-449.
44. Palumbo R, De Marchis F, Pusterla T, Conti A, Alessio M, Bianchi ME: **Src family kinases are necessary for cell migration induced by extracellular HMGB1.** *J Leukoc Biol* 2009, **86:**617-623.
45. Dumitriu IE, Bianchi ME, Bacci M, Manfredi AA, Rovere-Querini P: **The secretion of HMGB1 is required for the migration of maturing dendritic cells.** *J Leukoc Biol* 2007, **81:**84-91.
46. Vande Walle L, Kanneganti TD, Lamkanfi M: **HMGB1 release by inflammasomes.** *Virulence* 2011, **2:**162-165.
47. Lu B, Wang H, Andersson U, Tracey KJ: **Regulation of HMGB1 release by inflammasomes.** *Protein Cell* 2013, **4:**163-167.
48. Fiuza C, Bustin M, Talwar S, Tropea M, Gerstenberger E, Shelhamer JH, Suffredini AF: **Inflammation-promoting activity of HMGB1 on human microvascular endothelial cells.** *Blood* 2003, **101:**2652-2660.
49. Rayavara K, Kurosky A, Stafford SJ, Garg NJ, Brasier AR, Garofalo RP, Hosakote YM: **Proinflammatory Effects of Respiratory Syncytial Virus–Induced Epithelial HMGB1 on Human Innate Immune Cell Activation.** *The Journal of Immunology* 2018, **201:**2753-2766.
50. Festoff BW, Sajja RK, van Dreden P, Cucullo L: **HMGB1 and thrombin mediate the blood-brain barrier dysfunction acting as biomarkers of neuroinflammation and progression to neurodegeneration in Alzheimer's disease.** *J Neuroinflammation* 2016, **13:**194.
51. Deng M, Scott MJ, Fan J, Billiar TR: **Location is the key to function: HMGB1 in sepsis and trauma-induced inflammation.** *J Leukoc Biol* 2019, **106:**161-169.

52. Zhang Q, Hu S, Wang K, Cui M, Li X, Wang M, Hu X: **Engineering a yeast double-molecule carrier for drug screening.** *Artif Cells Nanomed Biotechnol* 2018, **46:**386-396.

53. Lotze MT, Tracey KJ: **High-mobility group box 1 protein (HMGB1): nuclear weapon in the immune arsenal.** *Nat Rev Immunol* 2005, **5:**331-342.

54. Wang H, Ward MF, Fan XG, Sama AE, Li W: **Potential role of high mobility group box 1 in viral infectious diseases.** *Viral Immunol* 2006, **19:**3-9.

55. Gardella S, Andrei C, Ferrera D, Lotti LV, Torrisi MR, Bianchi ME, Rubartelli A: **The nuclear protein HMGB1 is secreted by monocytes via a non-classical, vesicle-mediated secretory pathway.** *EMBO Rep* 2002, **3:**995-1001.

56. Tsung A, Klune JR, Zhang X, Jeyabalan G, Cao Z, Peng X, Stolz DB, Geller DA, Rosengart MR, Billiar TR: **HMGB1 release induced by liver ischemia involves Toll-like receptor 4 dependent reactive oxygen species production and calcium-mediated signaling.** *J Exp Med* 2007, **204:**2913-2923.

57. Oh YJ, Youn JH, Ji Y, Lee SE, Lim KJ, Choi JE, Shin JS: **HMGB1 is phosphorylated by classical protein kinase C and is secreted by a calcium-dependent mechanism.** *J Immunol* 2009, **182:**5800-5809.

58. Shirasuna K, Seno K, Ohtsu A, Shiratsuki S, Ohkuchi A, Suzuki H, Matsubara S, Nagayama S, Iwata H, Kuwayama T: **AGEs and HMGB1 Increase Inflammatory Cytokine Production from Human Placental Cells, Resulting in an Enhancement of Monocyte Migration.** *Am J Reprod Immunol* 2016, **75:**557-568.

59. Sweeney MD, Zhao Z, Montagne A, Nelson AR, Zlokovic BV: **Blood-Brain Barrier: From Physiology to Disease and Back.** *Physiol Rev* 2019, **99:**21-78.

60. Al-Obaidi MMJ, Bahadoran A, Wang SM, Manikam R, Raju CS, Sekaran SD: **Disruption of the blood brain barrier is vital property of neurotropic viral infection of the central nervous system.** *Acta Virol* 2018, **62:**16-27.

61. Lim SM, Koraka P, Osterhaus AD, Martina BE: **West Nile virus: immunity and pathogenesis.** *Viruses* 2011, **3:**811-828.

62. Verma S, Lo Y, Chapagain M, Lum S, Kumar M, Gurjav U, Luo H, Nakatsuka A, Nerurkar VR: **West Nile virus infection modulates human brain microvascular endothelial cells tight junction proteins and cell adhesion molecules: Transmigration across the in vitro blood-brain barrier.** *Virology* 2009, **385:**425-433.

63. Wang K, Wang H, Lou W, Ma L, Li Y, Zhang N, Wang C, Li F, Awais M, Cao S, et al: **IP-10 Promotes Blood-Brain Barrier Damage by Inducing Tumor Necrosis Factor Alpha Production in Japanese Encephalitis.** *Front Immunol* 2018, **9:**1148.

64. Helms HC, Abbott NJ, Burek M, Cecchelli R, Couraud PO, Deli MA, Forster C, Galla HJ, Romero IA, Shusta EV, et al: **In vitro models of the blood-brain barrier: An overview of commonly used brain endothelial cell culture models and guidelines for their use.** *J Cereb Blood Flow Metab* 2016, **36:**862-890.

65. Man S, Tucky B, Cotleur A, Drazba J, Takeshita Y, Ransohoff RM: **CXCL12-induced monocyte-endothelial interactions promote lymphocyte transmigration across an in vitro blood-brain barrier.** *Sci Transl Med* 2012, **4:**119ra114.

66. Netland J, Bevan MJ: **CD8 and CD4 T cells in west nile virus immunity and pathogenesis.** *Viruses* 2013, **5:**2573-2584.
67. Fu TL, Ong KC, Tan SH, Wong KT: **Japanese Encephalitis Virus Infects the Thalamus Early Followed by Sensory-Associated Cortex and Other Parts of the Central and Peripheral Nervous Systems.** *J Neuropathol Exp Neurol* 2019, **78:**1160-1170.

Figures

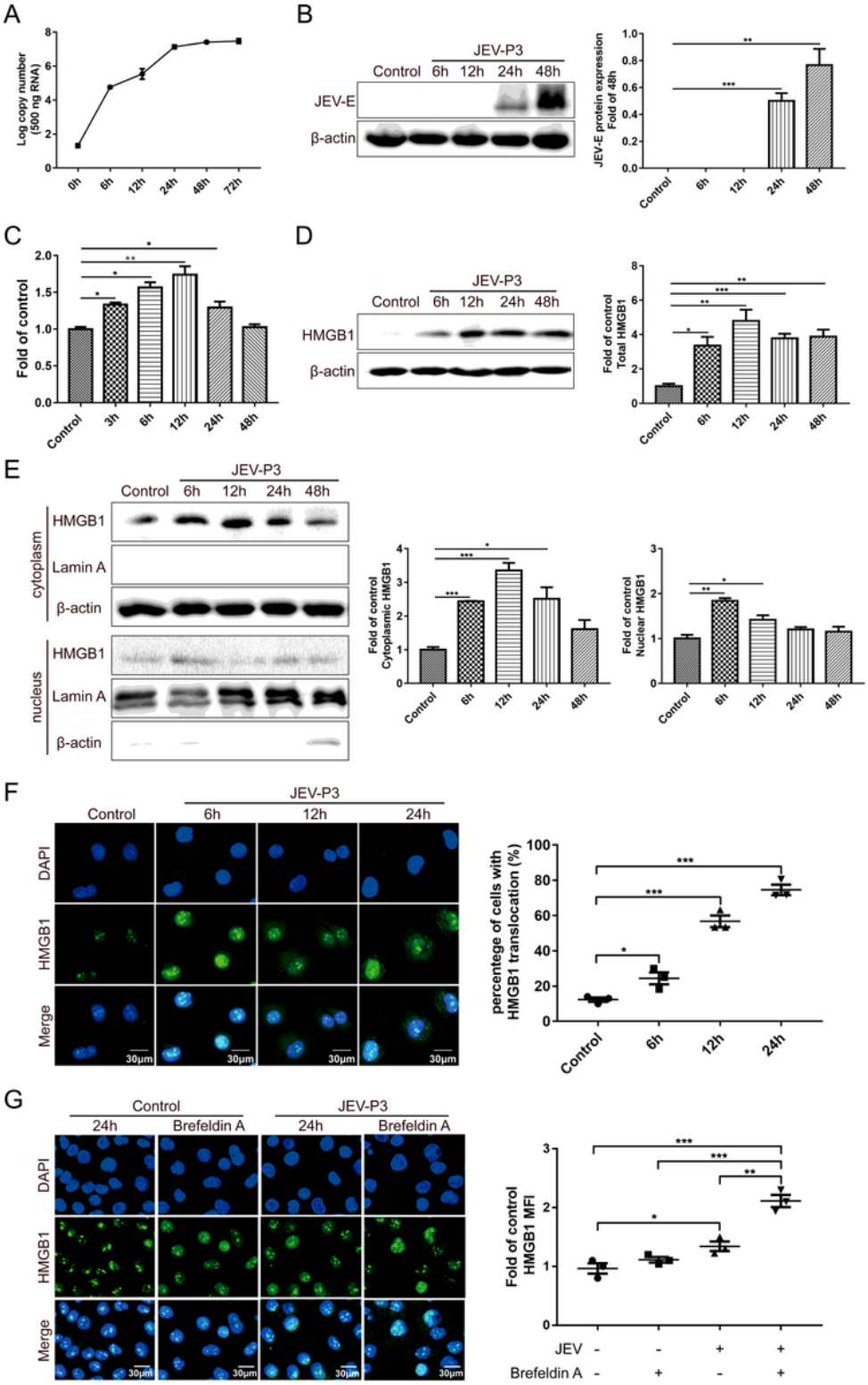

Figure 1

JEV induced HMGB1 fluctuation in HBMEC. HBMECs were infected with JEV-P3 at MOI of 1, and total cell protein was harvested at indicated times to measure JEV replication in HBMEC by real-time PCR (A) and Western blotting using anti-JEV-E protein antibody (B). mRNA (C) and Western blotting (D) analysis of HMGB1 levels at indicated times during JEV infection. JEV infected cells were normalized to uninfected cells for each post-infection time. (E) Total cell cytoplasmic and nuclear protein were extracted from JEV-

infected HBMEC at 0 h, 6 h, 12 h, 24 h, 48 h and 72 h postinfection. HMGB1 and Lamin A protein were measured by western blotting, wherein beta-actin acted as an internal control for protein integrity and lamin A was used for nuclear extraction. (F) HBMEC were infected or non-infected with JEV-P3, and the cells were incubated for 6 h, 12 h and 24 h with anti-HMGB1 polyclonal antibody followed by FITC-conjugated secondary antibody, then imaged by immunofluorescence staining for DNA (blue, DAPI), HMGB1 (green), and IF assay showed the translocation of HMGB1 in HBMECs. (G) HBMECs were infected with JEV-P3 for 12 h, following a co-incubation with Brefeldin A (Golgi vesicles inhibitor), then imaging by immunofluorescence staining for DNA (DAPI, blue), HMGB1 (green) at 24 h. Followed with the statistical analysis of HMGB1 (MFI) in HBMECs. Virus uninfected cells were acted as control. These data were repeated at least three times. Scale bar for (E) (G) is 30 μm. These data were expressed as the means ± SEM. *$p < 0.05$; **$p < 0.01$, ***$p < 0.001$.

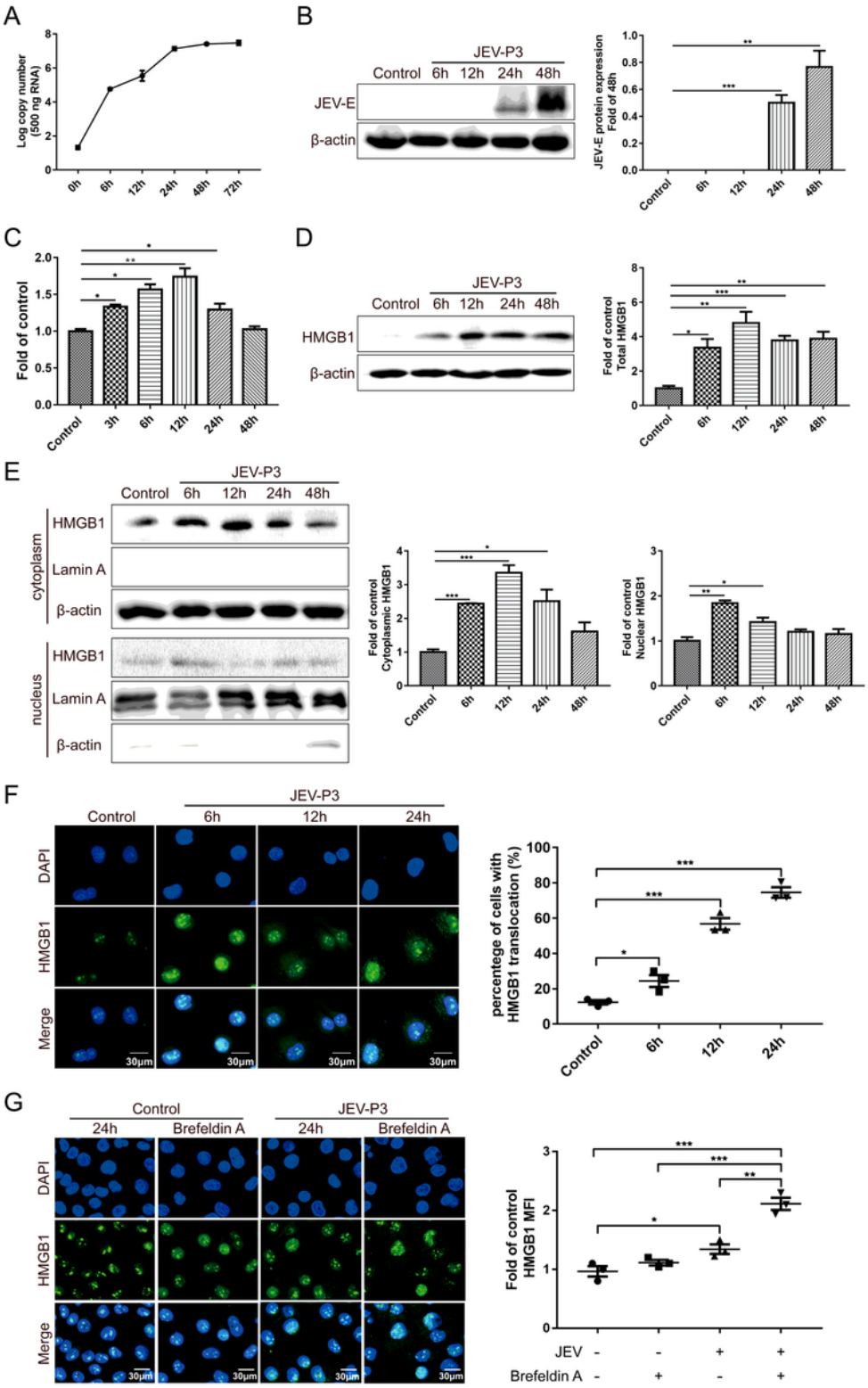

Figure 1

JEV induced HMGB1 fluctuation in HBMEC. HBMECs were infected with JEV-P3 at MOI of 1, and total cell protein was harvested at indicated times to measure JEV replication in HBMEC by real-time PCR (A) and Western blotting using anti-JEV-E protein antibody (B). mRNA (C) and Western blotting (D) analysis of HMGB1 levels at indicated times during JEV infection. JEV infected cells were normalized to uninfected cells for each post-infection time. (E) Total cell cytoplasmic and nuclear protein were extracted from JEV-

infected HBMEC at 0 h, 6 h, 12 h, 24 h, 48 h and 72 h postinfection. HMGB1 and Lamin A protein were measured by western blotting, wherein beta-actin acted as an internal control for protein integrity and lamin A was used for nuclear extraction. (F) HBMEC were infected or non-infected with JEV-P3, and the cells were incubated for 6 h, 12 h and 24 h with anti-HMGB1 polyclonal antibody followed by FITC-conjugated secondary antibody, then imaged by immunofluorescence staining for DNA (blue, DAPI), HMGB1 (green), and IF assay showed the translocation of HMGB1 in HBMECs. (G) HBMECs were infected with JEV-P3 for 12 h, following a co-incubation with Brefeldin A (Golgi vesicles inhibitor), then imaging by immunofluorescence staining for DNA (DAPI, blue), HMGB1 (green) at 24 h. Followed with the statistical analysis of HMGB1 (MFI) in HBMECs. Virus uninfected cells were acted as control. These data were repeated at least three times. Scale bar for (E) (G) is 30 μm. These data were expressed as the means ± SEM. *$p < 0.05$; **$p < 0.01$, ***$p < 0.001$.

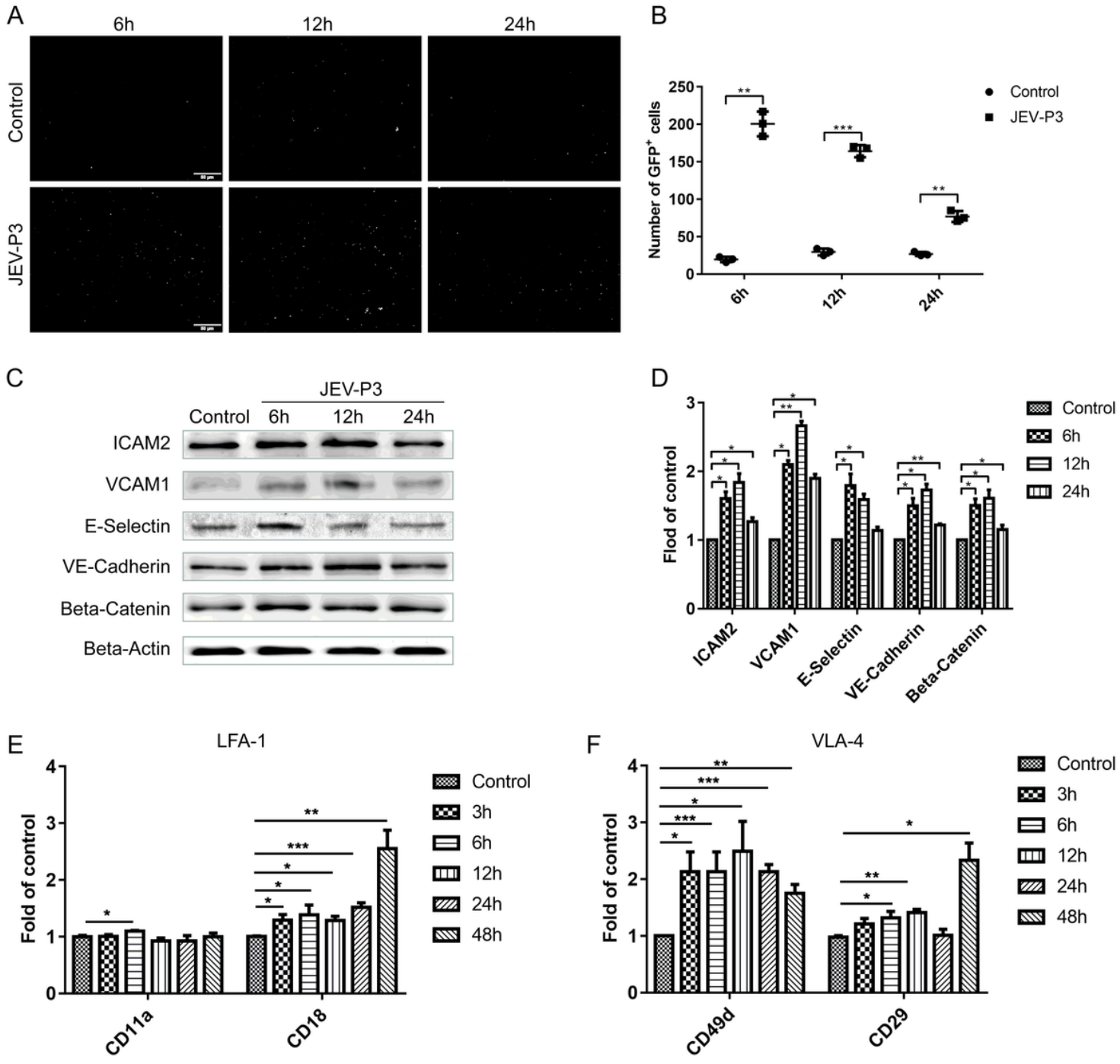

Figure 2

JEV caused fluctuation of adhesion molecules on bEnd.3 monolayer and rHMGB1 upregulated integrin ligands of splenocytes. (A) Representative images showing the extent of high expression of GFP-LFA-1-yeast. (B) Statistical fluorescence was used to represent the expression levels of ICAM-1. (C) ICAM-2, E-Selectin (CD62E), VE-Cadherin, Beta-Catenin levels in bEnd.3 cells, which were exposed to JEV-P3 and measured by western blotting, wherein beta-actin acted as the control. Protein samples were collected at indicated times (0 h, 6 h, 12 h, 24 h). (D) Protein expressions of the panel (C) were normalized to beta-actin, which were respectively and quantitatively analyzed as the related fold fluctuation to the control. Expression levels of LFA-1(CD11a and CD18) (E) and VLA-4 (CD49d and CD29) (F) in recombinant

HMGB1-treated (100 ng/ml) mice splenocytes, which were performed by real-time PCR at indicated times (0 h, 3 h, 6 h, 12 h, 24 h, 48 h). These data were repeated at least three times. These data were expressed as the means ± SEM. *p < 0.05; **p < 0.01, ***p < 0.001.

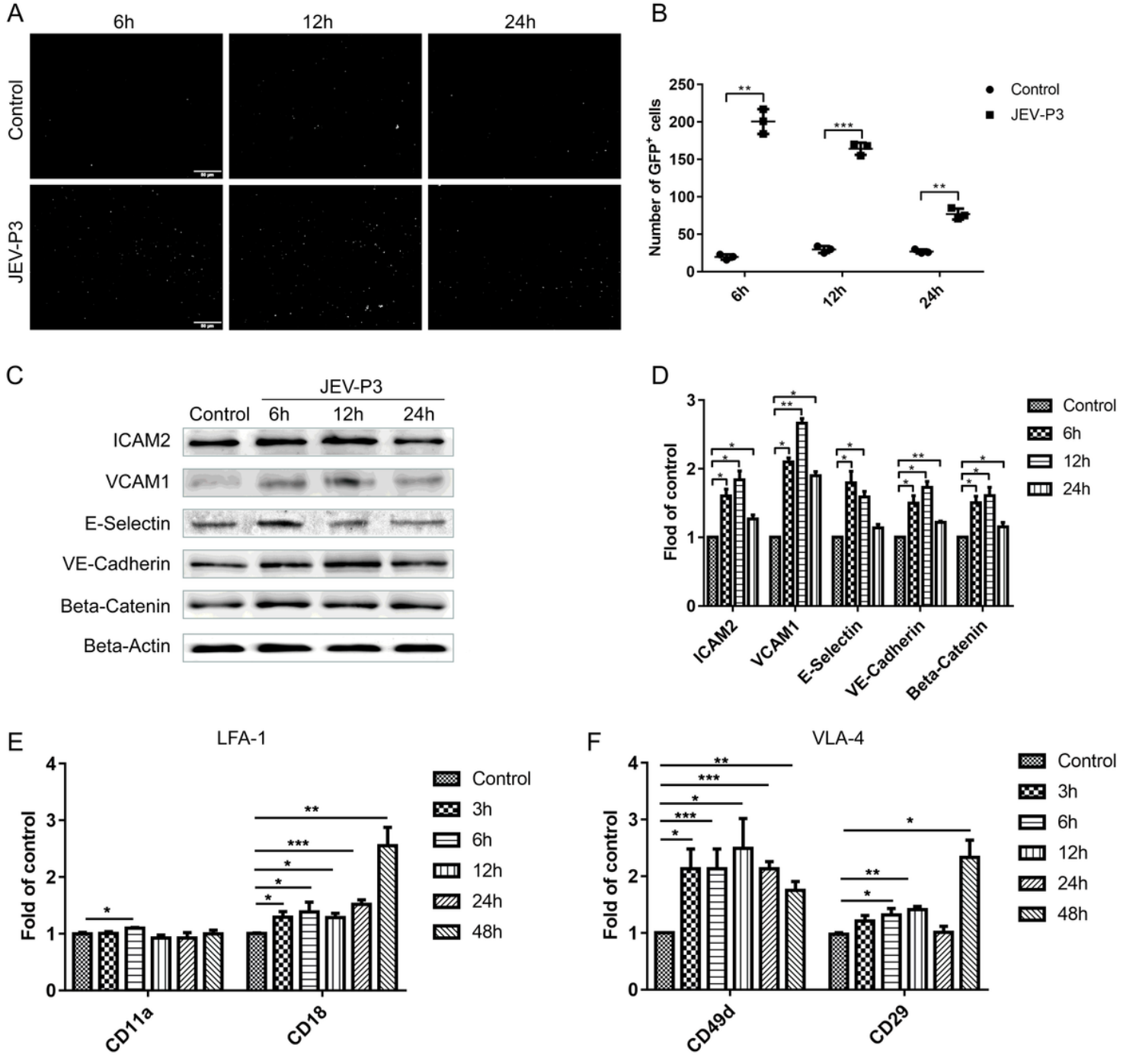

Figure 2

JEV caused fluctuation of adhesion molecules on bEnd.3 monolayer and rHMGB1 upregulated integrin ligands of splenocytes. (A) Representative images showing the extent of high expression of GFP-LFA-1-yeast. (B) Statistical fluorescence was used to represent the expression levels of ICAM-1. (C) ICAM-2, E-Selectin (CD62E), VE-Cadherin, Beta-Catenin levels in bEnd.3 cells, which were exposed to JEV-P3 and measured by western blotting, wherein beta-actin acted as the control. Protein samples were collected at

indicated times (0 h, 6 h, 12 h, 24 h). (D) Protein expressions of the panel (C) were normalized to beta-actin, which were respectively and quantitatively analyzed as the related fold fluctuation to the control. Expression levels of LFA-1(CD11a and CD18) (E) and VLA-4 (CD49d and CD29) (F) in recombinant HMGB1-treated (100 ng/ml) mice splenocytes, which were performed by real-time PCR at indicated times (0 h, 3 h, 6 h, 12 h, 24 h, 48 h). These data were repeated at least three times. These data were expressed as the means ± SEM. *p < 0.05; **p < 0.01, ***p < 0.001.

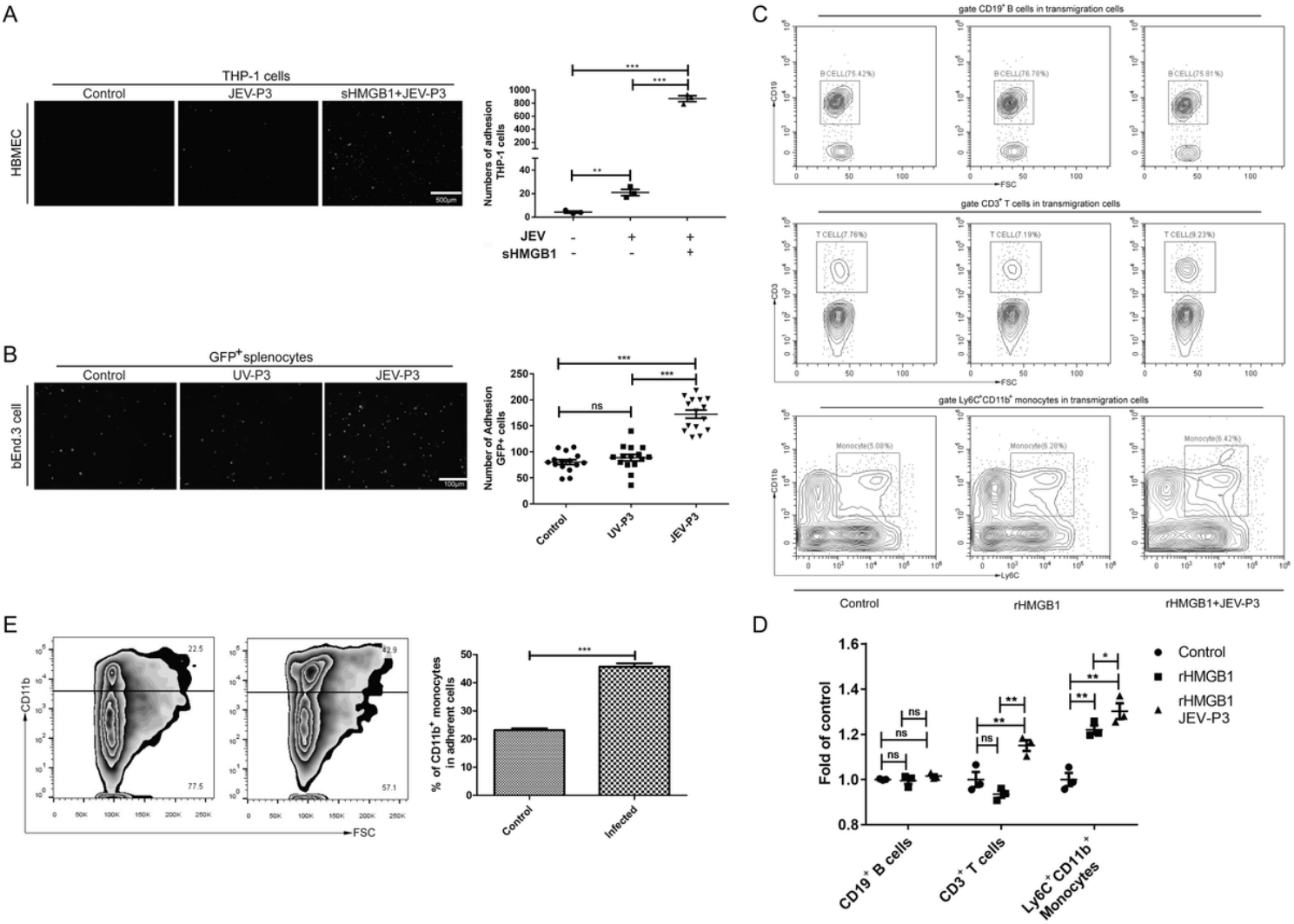

Figure 3

HMGB1 promoted immune cells adhesion to the BMEC monolayer. (A) THP-1 cells were treated with sHMGB1 (supernatant HMGB1), or sHMGB1 and TSA. BMEC monolayers were co-cultured with THP-1 cells and mice splenocytes for 2 h. The monolayers were washed by PBS and fixed with 4% paraformaldehyde, immunostained with anti-CD14 and FITC-labeled secondary antibody and then were observed by fluorescence microscope. (B) JEV-P3/UV-P3 infected bEnd.3 cell monolayers were co-cultured with GFP+-splenocytes for 2 h, which were isolated from GFP+-mice. JEV-free bEnd.3 cell monolayers were acting as the control. The fluorescence represents the number of adherent spleen cells, which were observed by fluorescence microscope. (C) Mice splenocytes were treated with rHMGB1 (100 ng/ml) for 2 h. Then, co-cultured with bEnd.3 cells monolayers for 2 h. Washed by PBS and then

adhesion splenocytes were collected and stained by flow antibody for the detection of CD19+ B cells, CD3+ T cells and Ly6C+CD11b+ monocytes. (D) Statistics of adhesion splenocytes to the bEnd.3 cells monolayer of (C). (E) The purified Ly6C+ monocytes were co-cultured with JEV-infected bEnd.3 cells monolayer for 2 h. After washing by PBS, collect the binding monocytes and performby flow cytometry. Scale bar for (A) and (B) is 500 μm and 100 μm. These data were repeated at least three times. These data were expressed as the means ± SEM. *p < 0.05; **p < 0.01, ***p < 0.001.

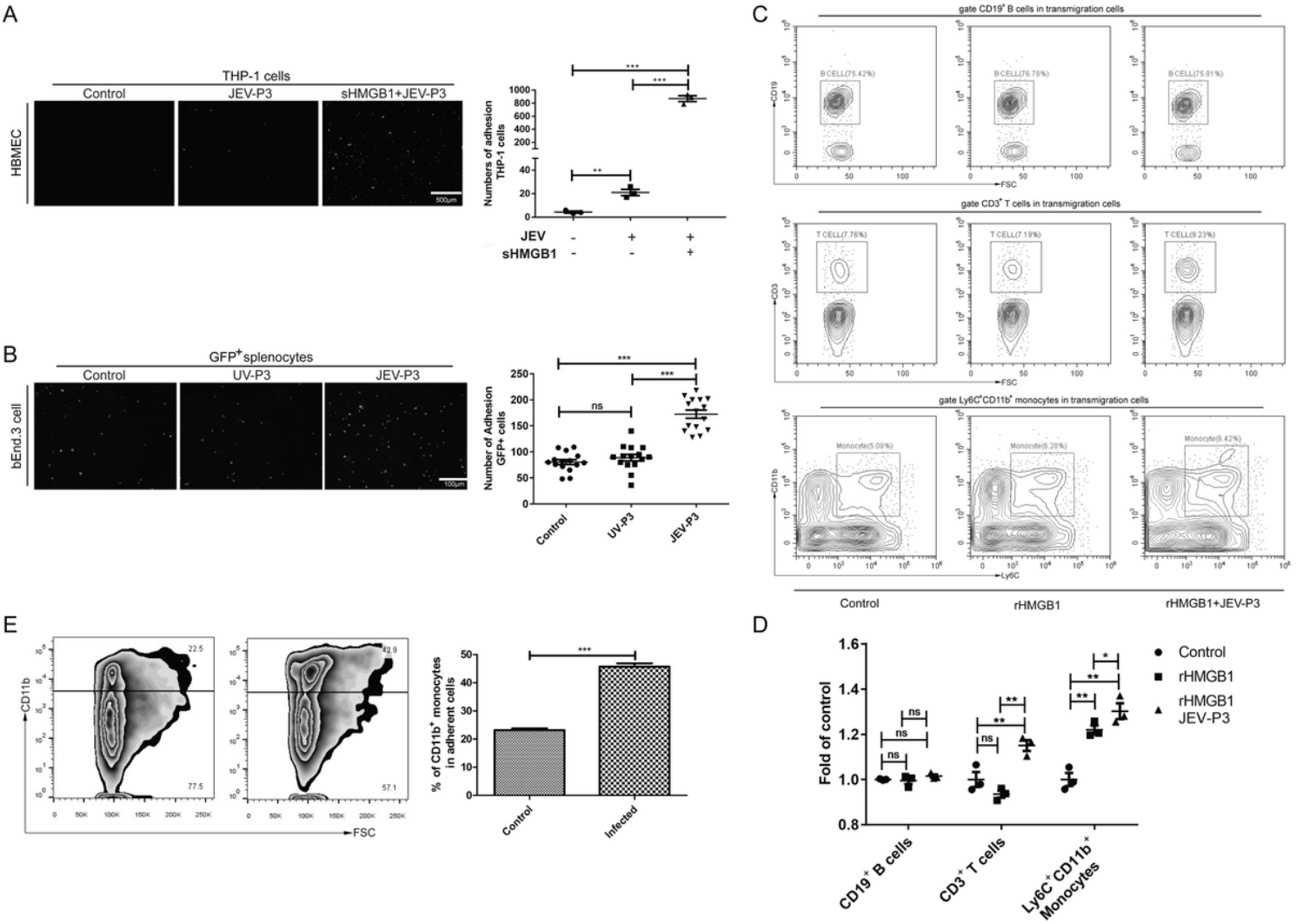

Figure 3

HMGB1 promoted immune cells adhesion to the BMEC monolayer. (A) THP-1 cells were treated with sHMGB1 (supernatant HMGB1), or sHMGB1 and TSA. BMEC monolayers were co-cultured with THP-1 cells and mice splenocytes for 2 h. The monolayers were washed by PBS and fixed with 4% paraformaldehyde, immunostained with anti-CD14 and FITC-labeled secondary antibody and then were observed by fluorescence microscope. (B) JEV-P3/UV-P3 infected bEnd.3 cell monolayers were co-cultured with GFP+-splenocytes for 2 h, which were isolated from GFP+-mice. JEV-free bEnd.3 cell monolayers were acting as the control. The fluorescence represents the number of adherent spleen cells, which were observed by fluorescence microscope. (C) Mice splenocytes were treated with rHMGB1 (100 ng/ml) for 2 h. Then, co-cultured with bEnd.3 cells monolayers for 2 h. Washed by PBS and then

adhesion splenocytes were collected and stained by flow antibody for the detection of CD19+ B cells, CD3+ T cells and Ly6C+CD11b+ monocytes. (D) Statistics of adhesion splenocytes to the bEnd.3 cells monolayer of (C). (E) The purified Ly6C+ monocytes were co-cultured with JEV-infected bEnd.3 cells monolayer for 2 h. After washing by PBS, collect the binding monocytes and performby flow cytometry. Scale bar for (A) and (B) is 500 μm and 100 μm. These data were repeated at least three times. These data were expressed as the means ± SEM. *p < 0.05; **p < 0.01, ***p < 0.001.

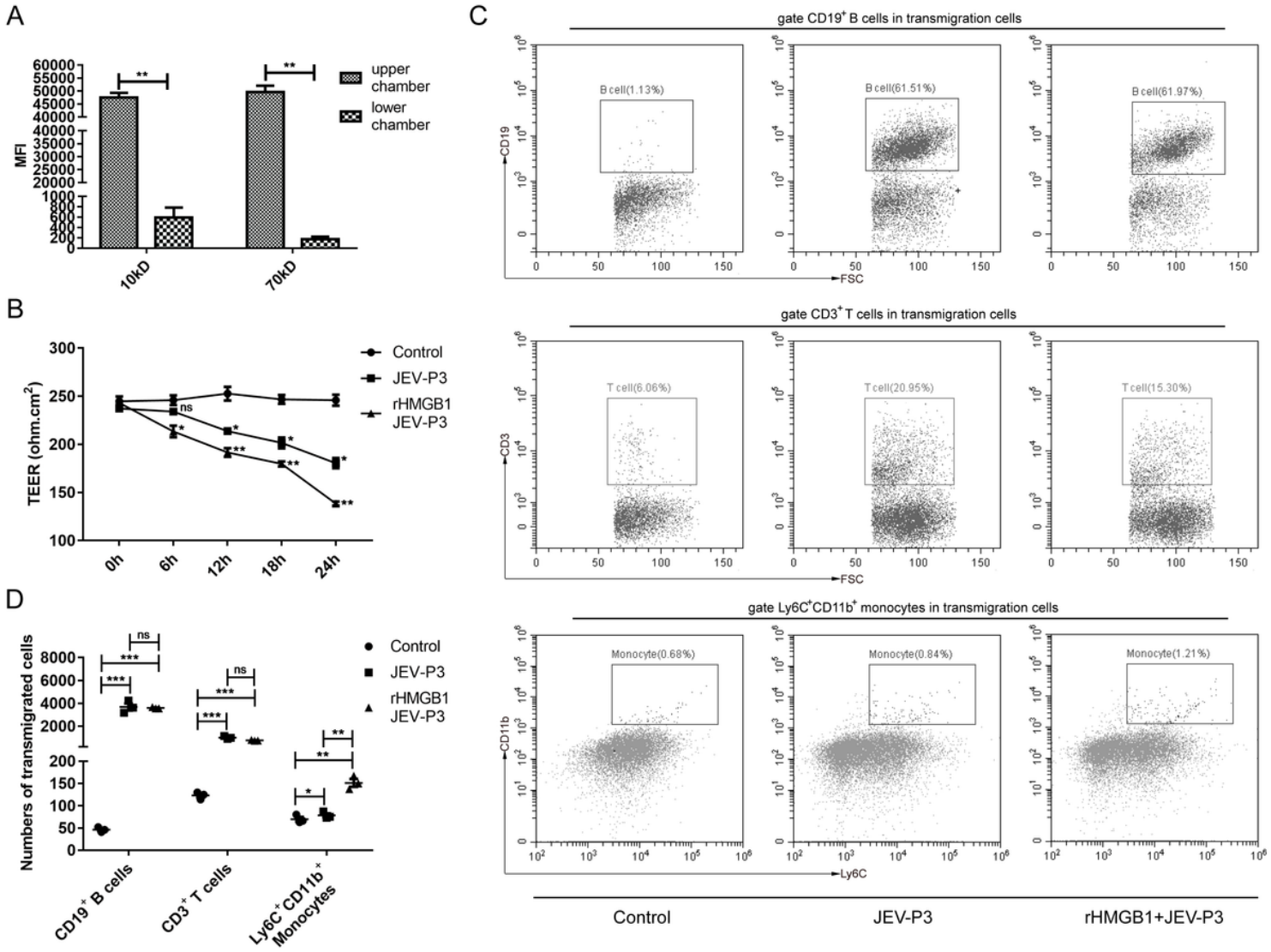

Figure 4

HMGB1 facilitated immune cells transmigration during early infection. bEnd.3 cells were cultured in the collagen-covered upper chamber in culture medium (no phenol red) for 24 h. Then, the permeability and TEER value of BMEC monolayer models were detected. Mice splenocytes (5×105) were added into the upper chamber and co-cultured with bEnd.3 cell monolayer for 24 h. Then collected transmigrated cells in the lower chamber and detected by flow cytometry. (A) FITC-dextran (10 kD and 70 kD) was added into the upper chamber. After 30 min, FITC-dextran (the upper chamber and the lower chamber) was collected for the detection of the fluorescence intensity by ELIASA. (B) bEnd.3 cells were cultured in the collagen-coated upper chamber for 24 h. The measurement of the TEER value of control, JEV-P3 (Mice

splenocytes and JEV-infected monolayer) and rHMGB1-JEV-P3 (rHMGB1 treated splenocytes and JEV-infected monolayer) monolayer models at indicated times (0 h, 6 h, 12 h, 18 h, 24 h). (C) After bEnd.3 cell monolayer was treated with JEV at MOI of 1 for 2 h, it was then co-cultured with splenocytes or rHMGB1-treated splenocytes (5×105) for 24 h, transmigrated cells (lower chamber) were collected and measured by flow cytometry, including CD19+ B cells, CD3+ T cells and Ly6C+CD11b+ monocytes. (D) Statistics of transmigration cells in the lower chamber of (C). These data were repeated at least three times. These data were expressed as the means ± SEM. *p < 0.05; **p < 0.01, ***p < 0.001.

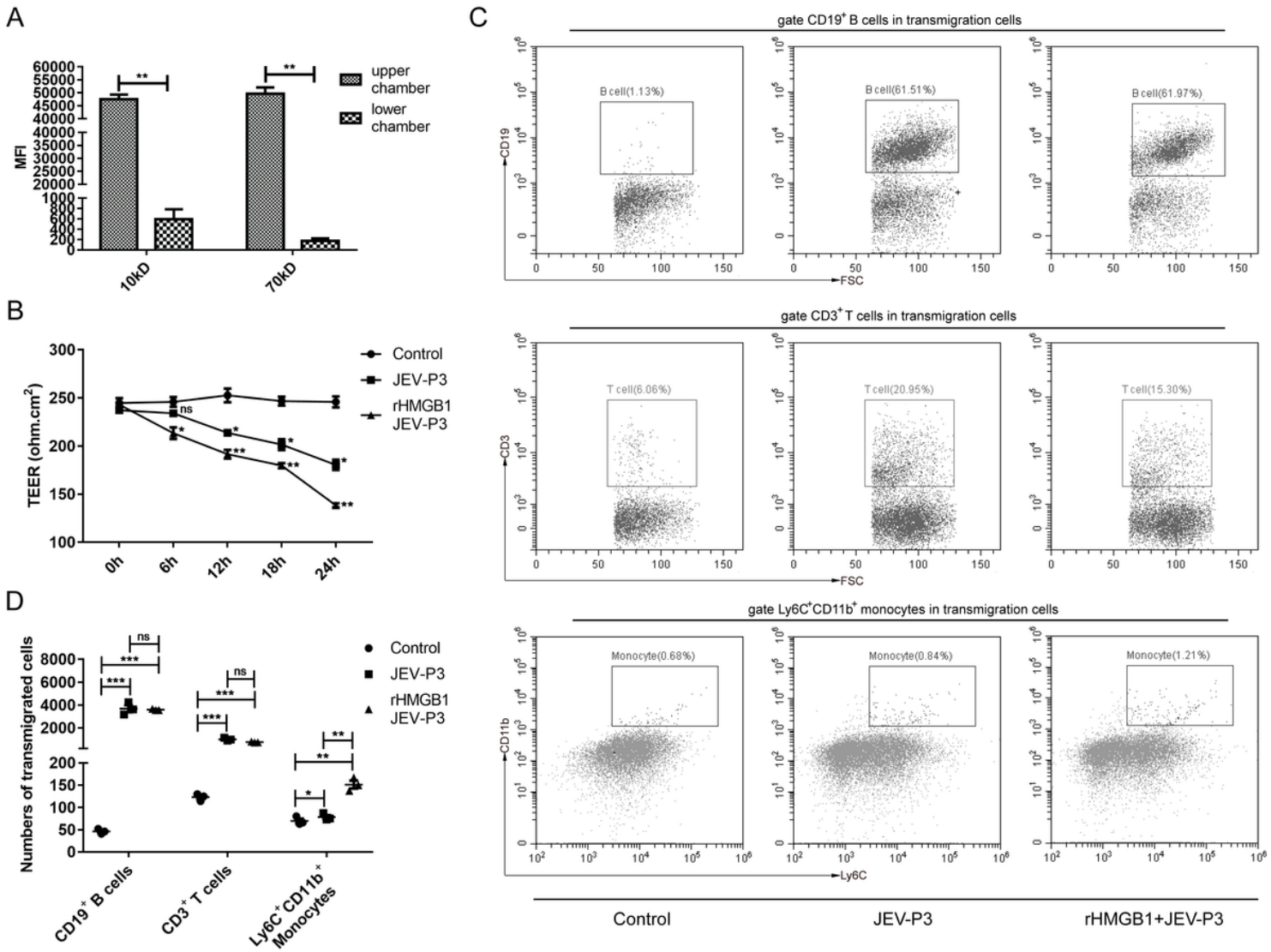

Figure 4

HMGB1 facilitated immune cells transmigration during early infection. bEnd.3 cells were cultured in the collagen-covered upper chamber in culture medium (no phenol red) for 24 h. Then, the permeability and TEER value of BMEC monolayer models were detected. Mice splenocytes (5×105) were added into the upper chamber and co-cultured with bEnd.3 cell monolayer for 24 h. Then collected transmigrated cells in the lower chamber and detected by flow cytometry. (A) FITC-dextran (10 kD and 70 kD) was added into the upper chamber. After 30 min, FITC-dextran (the upper chamber and the lower chamber) was collected for the detection of the fluorescence intensity by ELIASA. (B) bEnd.3 cells were cultured in the collagen-

coated upper chamber for 24 h. The measurement of the TEER value of control, JEV-P3 (Mice splenocytes and JEV-infected monolayer) and rHMGB1-JEV-P3 (rHMGB1 treated splenocytes and JEV-infected monolayer) monolayer models at indicated times (0 h, 6 h, 12 h, 18 h, 24 h). (C) After bEnd.3 cell monolayer was treated with JEV at MOI of 1 for 2 h, it was then co-cultured with splenocytes or rHMGB1-treated splenocytes (5×105) for 24 h, transmigrated cells (lower chamber) were collected and measured by flow cytometry, including CD19+ B cells, CD3+ T cells and Ly6C+CD11b+ monocytes. (D) Statistics of transmigration cells in the lower chamber of (C). These data were repeated at least three times. These data were expressed as the means ± SEM. *$p < 0.05$; **$p < 0.01$, ***$p < 0.001$.

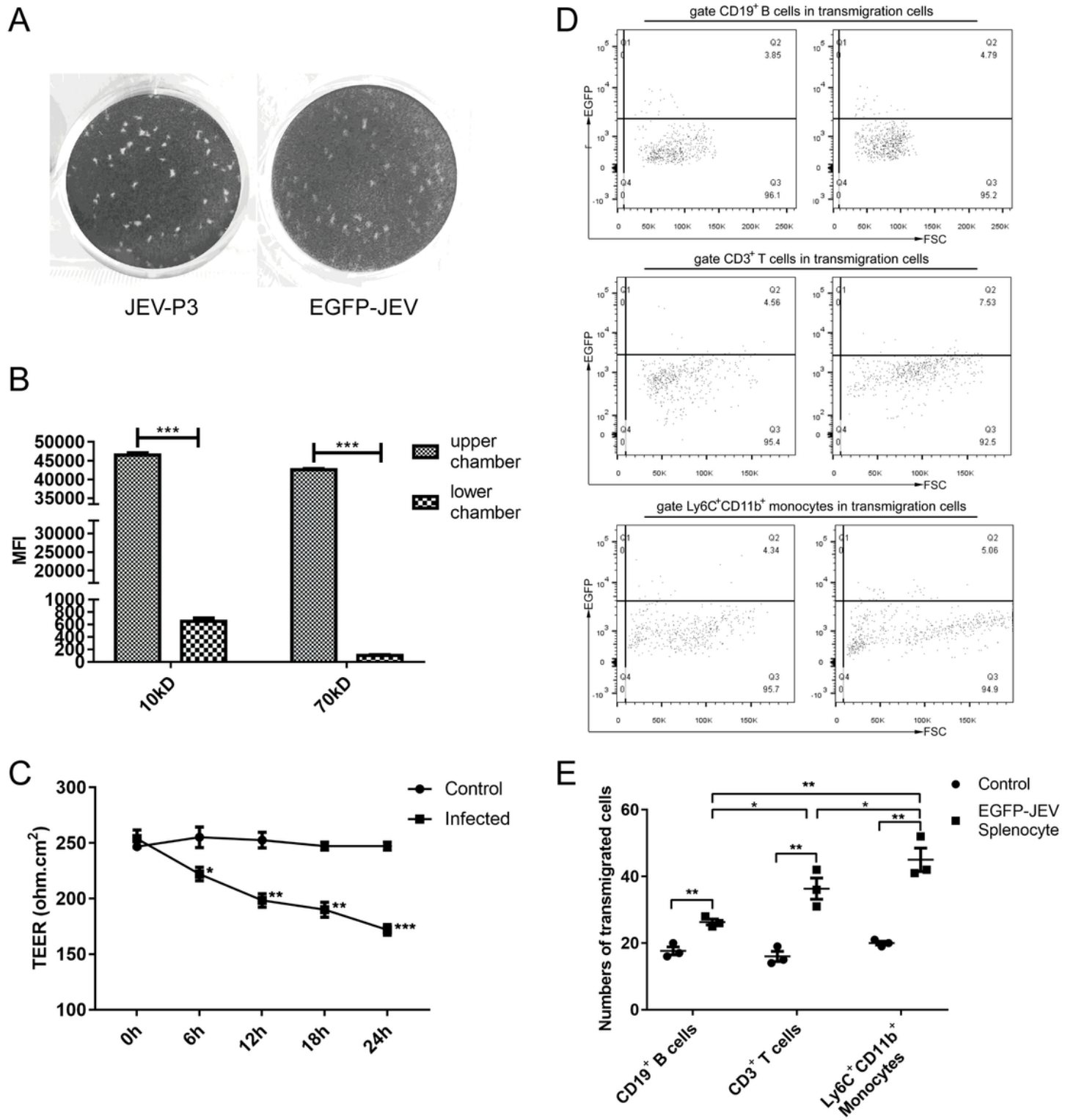

Figure 5

Evaluation of the monolayer model and immune cells transmigration. (A) Plaque morphology of eGFP-JEV is similar to JEV-P3 in BHK-21 cells. (B) The addition of FITC-dextran (10 kD and 70 kD) into the upper chamber. After 30 min, the fluorescence intensity of FITC-dextran in the upper and lower chamber was collected and detected by ELIASA. (C) The measurement of the TEER value of virus-infected and uninfected monolayer models at indicated times (0 h, 6 h, 12 h,18 h, 24 h). bEnd.3 cells were cultured in

the collagen-coated upper chamber. (D) JEV-infected bEnd.3 cell monolayer co-cultured with EGFP-JEV infected splenocytes (5×105) for 24 h, transmigrated cells (lower chamber) were collected and measured by flow cytometry. The enhanced sensitivity of 488 nm was utilized in the detection of intracellular EGFP-JEV in CD19+ B cells, CD3+ T cells and Ly6C+CD11b+ monocytes. (E) Statistics of transmigration EGFP-JEV infected cells in the lower chamber of (D). These data were repeated at least three times. These data were expressed as the means ± SEM. *p < 0.05; **p < 0.01, ***p < 0.001.

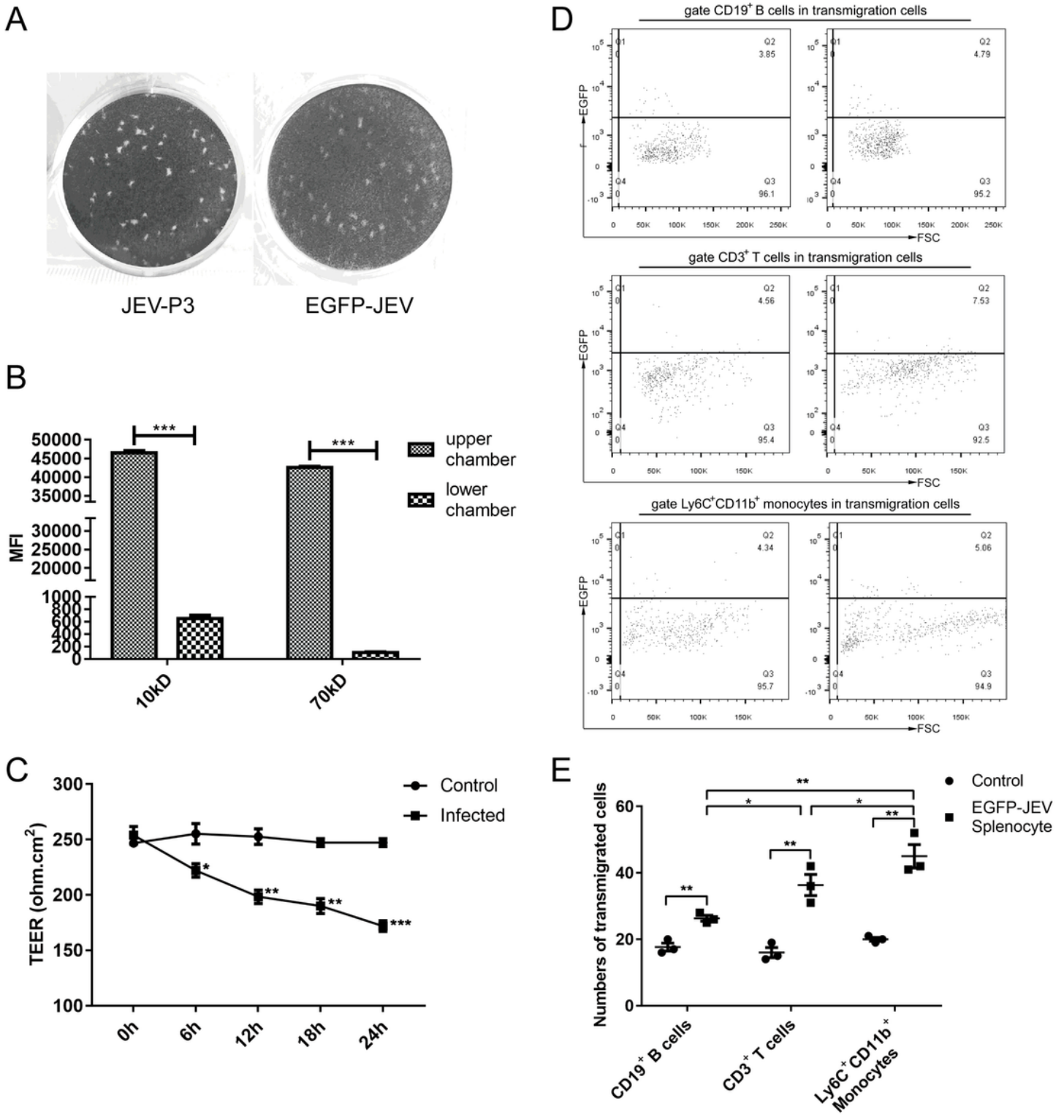

Figure 5

Evaluation of the monolayer model and immune cells transmigration. (A) Plaque morphology of eGFP-JEV is similar to JEV-P3 in BHK-21 cells. (B) The addition of FITC-dextran (10 kD and 70 kD) into the upper chamber. After 30 min, the fluorescence intensity of FITC-dextran in the upper and lower chamber was collected and detected by ELIASA. (C) The measurement of the TEER value of virus-infected and uninfected monolayer models at indicated times (0 h, 6 h, 12 h,18 h, 24 h). bEnd.3 cells were cultured in the collagen-coated upper chamber. (D) JEV-infected bEnd.3 cell monolayer co-cultured with EGFP-JEV infected splenocytes (5×105) for 24 h, transmigrated cells (lower chamber) were collected and measured by flow cytometry. The enhanced sensitivity of 488 nm was utilized in the detection of intracellular EGFP-JEV in CD19+ B cells, CD3+ T cells and Ly6C+CD11b+ monocytes. (E) Statistics of transmigration EGFP-JEV infected cells in the lower chamber of (D). These data were repeated at least three times. These data were expressed as the means ± SEM. *p < 0.05; **p < 0.01, ***p < 0.001.

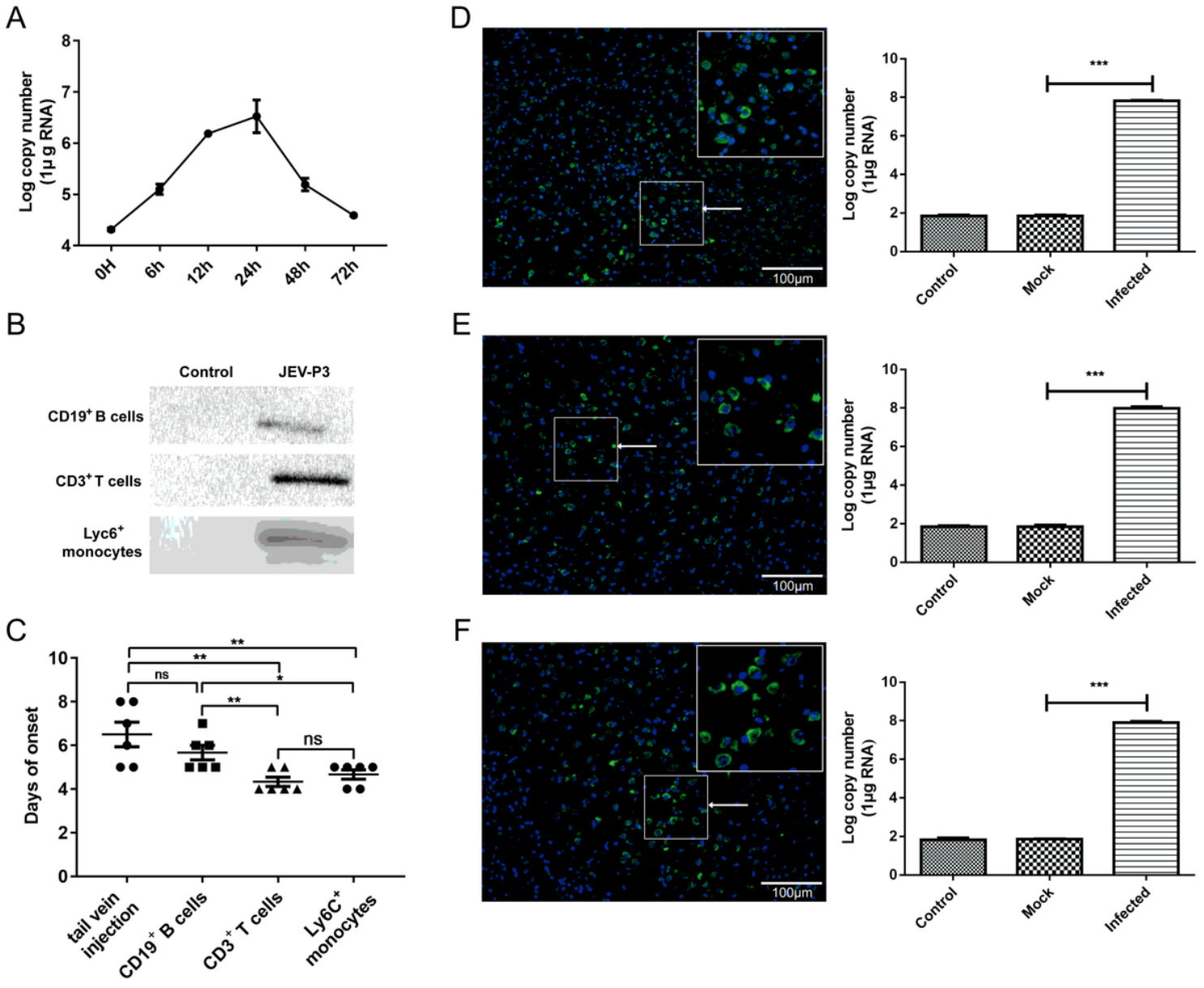

Figure 6

The presentation of JEV-infected immune cells in the CNS were affiliated to JE in mice. (A) The replication of JEV in mice splenocytes from 0 to 72 h, which were measured by real-time PCR. (B) CD3+ T cells, CD19+ B cells and Lyc6+ monocytes were exposed to JEV-P3, which were detected by western blotting using JEV-E protein antibody. (C) The statistics of mice onset time after JEV-infected CD19+ B cells, CD3+ T cells and Lyc6C+ monocytes were injected into healthy adult mice brain, compared to the tail vein injection group. After the injection of JEV-infected or uninfected (Mock) Ly6C+ monocytes (D), CD3+ T cells (E), CD19+ B cells. (F) Immunofluorescent images of JEV measurement of the JE mice brains, which were shown by staining for DNA (blue, DAPI) and JEV (green, JEV-E protein). JEV replication in mice brain was measured by real-time PCR. Scale bar for (D, E, F) is 100μm. These data were expressed as the means ± SEM. *p < 0.05; **p < 0.01, ***p < 0.001.

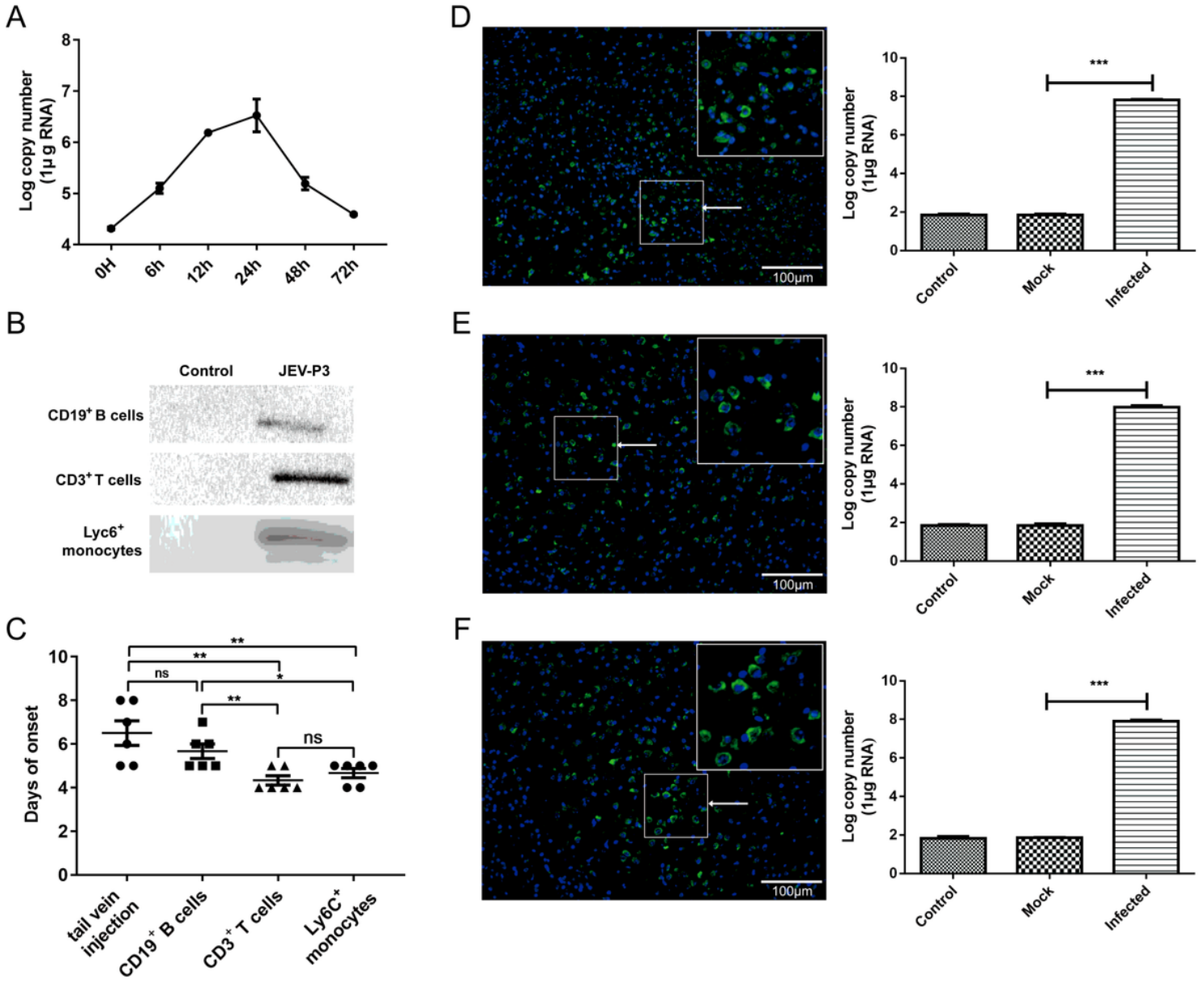

Figure 6

The presentation of JEV-infected immune cells in the CNS were affiliated to JE in mice. (A) The replication of JEV in mice splenocytes from 0 to 72 h, which were measured by real-time PCR. (B) CD3+ T cells, CD19+ B cells and Lyc6+ monocytes were exposed to JEV-P3, which were detected by western blotting using JEV-E protein antibody. (C) The statistics of mice onset time after JEV-infected CD19+ B cells, CD3+ T cells and Lyc6C+ monocytes were injected into healthy adult mice brain, compared to the tail vein injection group. After the injection of JEV-infected or uninfected (Mock) Ly6C+ monocytes (D), CD3+ T cells (E), CD19+ B cells. (F) Immunofluorescent images of JEV measurement of the JE mice brains, which were shown by staining for DNA (blue, DAPI) and JEV (green, JEV-E protein). JEV replication in mice brain was measured by real-time PCR. Scale bar for (D, E, F) is 100μm. These data were expressed as the means ± SEM. *p < 0.05; **p < 0.01, ***p < 0.001.

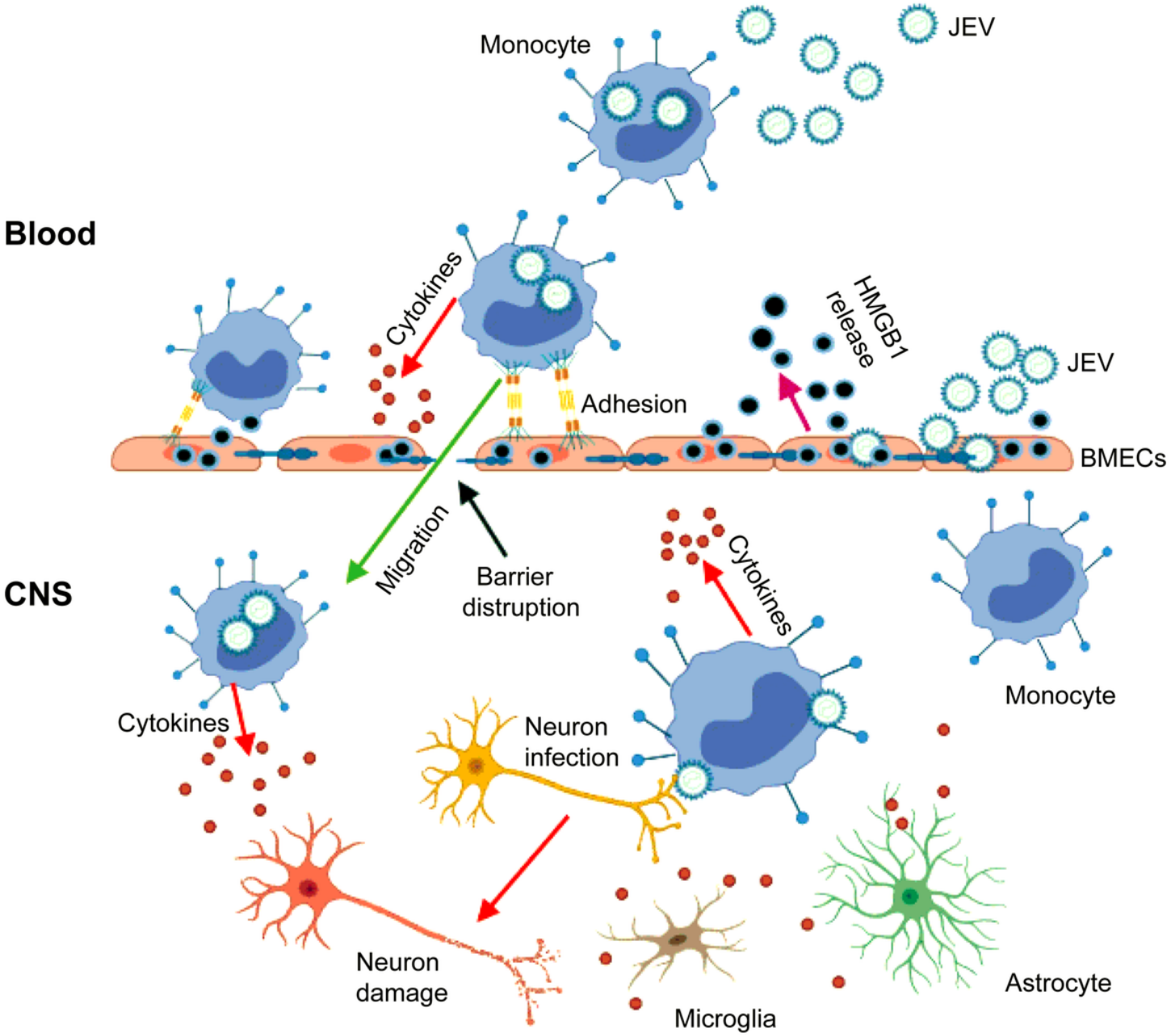

Figure 7

Schematic description of BMEC-derived HMGB1 contributes JEV-infected monocytes transendothelial migration. JEV induced HMGB1 release from brain microvascular endothelial cells and upregulated adhesion molecules, enhancing leukocyte-endothelium adhesion accompanied by promoted JEV-infected monocytes transendothelial migration and the fluctuation of BBB. JEV-infected monocytes acted as the “Trojan horse”, posing a positive effect on JE, glia activation and consequently expanding neuron infection, causing uncontrolled inflammation cytokines production and neuron damage, resulting in the appearance of JE symptoms earlier.

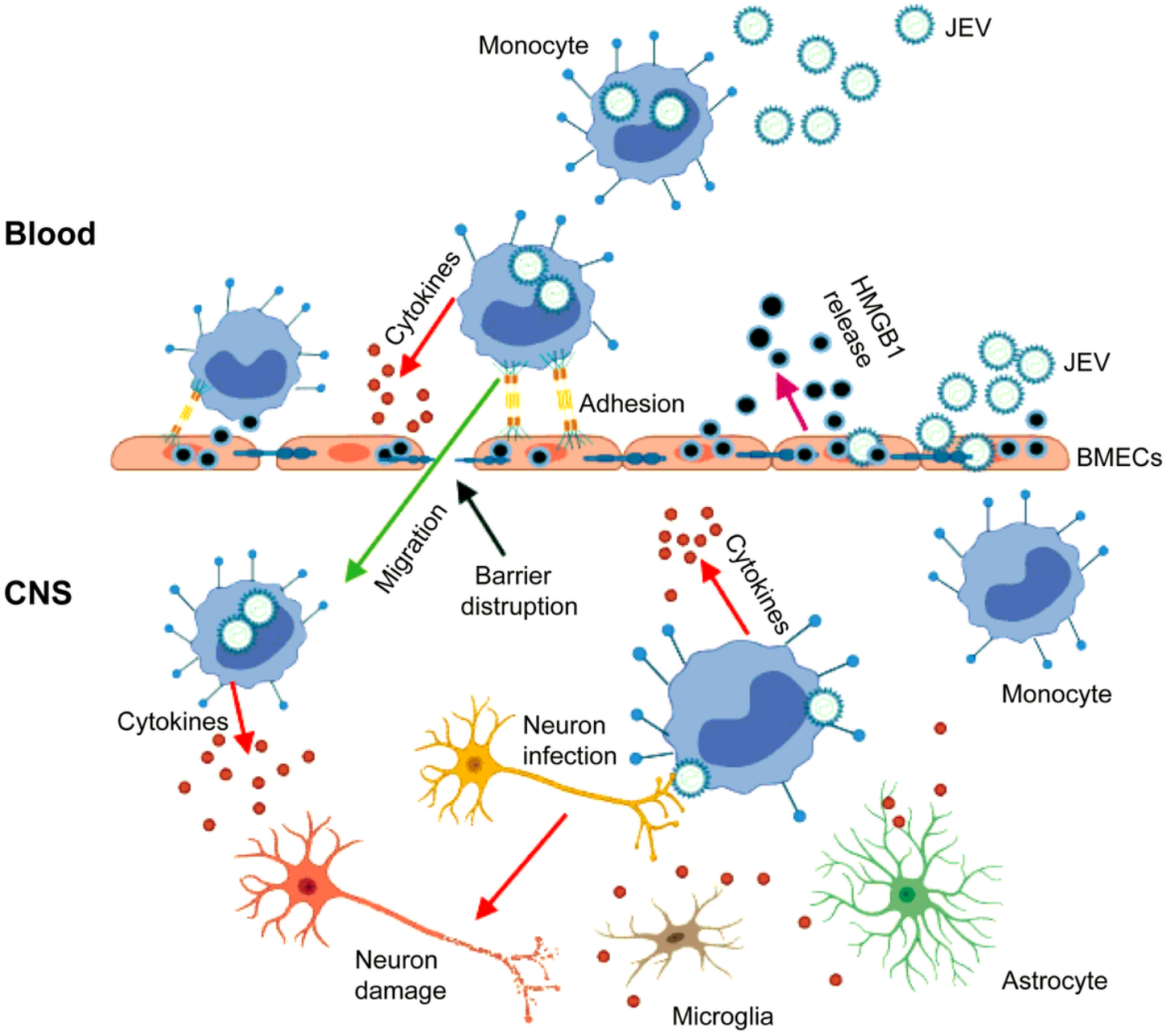

Figure 7

Schematic description of BMEC-derived HMGB1 contributes JEV-infected monocytes transendothelial migration. JEV induced HMGB1 release from brain microvascular endothelial cells and upregulated adhesion molecules, enhancing leukocyte-endothelium adhesion accompanied by promoted JEV-infected

monocytes transendothelial migration and the fluctuation of BBB. JEV-infected monocytes acted as the “Trojan horse”, posing a positive effect on JE, glia activation and consequently expanding neuron infection, causing uncontrolled inflammation cytokines production and neuron damage, resulting in the appearance of JE symptoms earlier.

Supplementary Files

This is a list of supplementary files associated with this preprint. Click to download.

- Supplementarymaterial.pdf
- Supplementarymaterial.pdf